

Soft Functionally Gradient Materials and Structures – Natural and Manmade: A Review

Akanksha Pragya and Tushar K. Ghosh*

Functionally gradient materials (FGM) have gradual variations in their properties along one or more dimensions due to local compositional or structural distinctions by design. Traditionally, hard materials (e.g., metals, ceramics) are used to design and fabricate FGMs; however, there is increasing interest in polymer-based soft and compliant FGMs mainly because of their potential application in the human environment. Soft FGMs are ideally suitable to manage interfacial problems in dissimilar materials used in many emerging devices and systems for human interaction, such as soft robotics and electronic textiles and beyond. Soft systems are ubiquitous in everyday lives; they are resilient and can easily deform, absorb energy, and adapt to changing environments. Here, the basic design and functional principles of biological FGMs and their manmade counterparts are discussed using representative examples. The remarkable multifunctional properties of natural FGMs resulting from their sophisticated hierarchical structures, built from a relatively limited choice of materials, offer a rich source of new design paradigms and manufacturing strategies for manmade materials and systems for emerging technological needs. Finally, the challenges and potential pathways are highlighted to leverage soft materials' facile processability and unique properties toward functional FGMs.

1. Introduction

Functionally gradient materials (FGM) are characterized by a gradual change in materials' bulk properties along one or more dimensions, see **Figure 1**. The varying properties enabled via compositional or structural manipulation at the macro-, micro-,

or nano-scales can involve but are not restricted to, mechanical, optical, electrical, magnetic, thermal, acoustic, wettability, etc. In general, the composition and structure of an FGM vary gradually and locally with no sharp interfaces. Based on the intended application, the gradient span (distance over which gradient occurs) can be concentrated within a small interface or be present throughout the bulk. Craftspeople have used gradient materials since the earliest times in the form of case-hardened steel that are still in common use today. However, it was only in 1972 that Shen and Bever first introduced the concept of the gradient in polymeric materials.^[1] Later in 1982, Wilson and Hutley studied the optically gradient groove profile in a moth's eye and fabricated one of the earliest replicas inspired by a naturally occurring gradient system.^[2] Ever since its inception, the interest in gradient materials has grown rapidly. Gradient structures have been used in diverse applications such as tissue engineering,^[3–7] prosthetics,^[8] implants,^[9] optics,^[10–12] actuation,^[13,14] aerospace,^[15,16] automation,^[17–19] etc. The concept of continuous variation in material properties is not a human invention; nature offers plenty of such examples that have enabled animal and plant species to survive and thrive in complex and dynamic environments. A plethora of natural gradient (herein termed bio-FGM) structures formed through millions of years of evolution and natural selection have been reported in the literature. These include a variety of examples, such as the mechanically gradient squid's beak^[20] and spruce trunk^[21] to optically gradient lenses in the human eyes.^[22] Scientists have continuously derived inspiration from bio-FGMs to fabricate manmade FGMs (herein, termed bioinspired FGMs) to fulfill complex and advanced applications. Other FGMs without any explicit bio-origin (herein, termed engineered FGMs) have also been prepared to fulfill certain application-specific requirements.

Several insightful reviews have been published in nearly four decades of its history on different aspects of functionally gradient materials and structures.^[23–30] While most of these reviews focus primarily on the mechanical behavior of FGMs, here we present a comprehensive overview of soft FGMs – both natural and manmade with mechanical, optical, electrical, magnetic, thermal, acoustic, and wettability gradients. Understanding the biological systems and the pathways through which nature

A. Pragya, T. K. Ghosh
 Department of Textile Engineering Chemistry and Science, Fiber, and
 Polymer Science Program
 Wilson College of Textiles
 North Carolina State University
 North Carolina State University
 1020 Main Campus Drive, Raleigh, NC 27606, USA
 E-mail: tghosh@ncsu.edu

 The ORCID identification number(s) for the author(s) of this article can be found under <https://doi.org/10.1002/adma.202300912>

© 2023 The Authors. Advanced Materials published by Wiley-VCH GmbH. This is an open access article under the terms of the Creative Commons Attribution-NonCommercial-NoDerivs License, which permits use and distribution in any medium, provided the original work is properly cited, the use is non-commercial and no modifications or adaptations are made.

DOI: [10.1002/adma.202300912](https://doi.org/10.1002/adma.202300912)

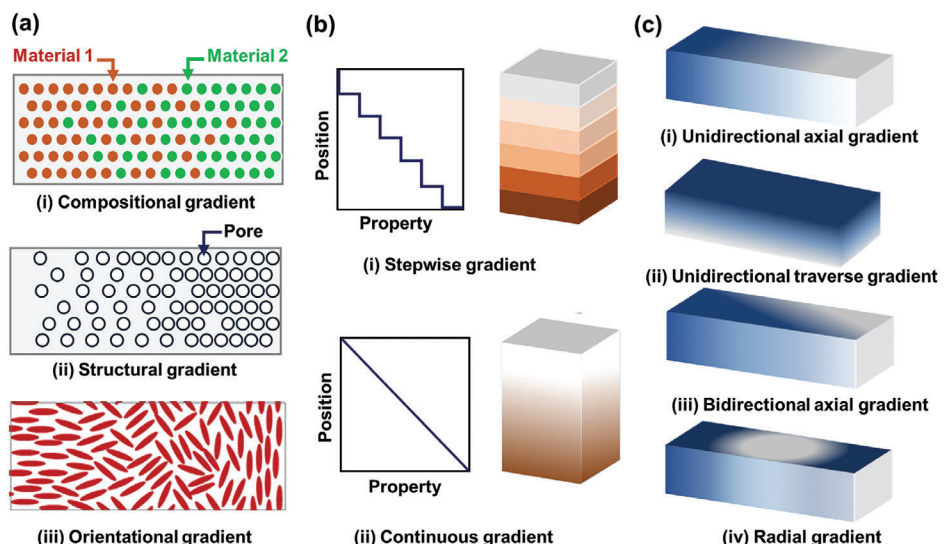


Figure 1. Schematic illustration of a) the different routes for the preparation of functionally gradient systems such as (i) compositional, (ii) structural (e.g., pores), and (iii) orientational (e.g., high aspect ratio particles), b) the gradient property transition (i) stepwise and (ii) continuous, and c) examples of the direction and dimensionality of the gradient, including, but not limited to (i) unidirectional axial, (ii) unidirectional transverse, (iii) bidirectional axial, and (iv) radial.

exploits the self-organization of materials, producing gradient systems for structural and functional performance is likely to stimulate new ideas toward novel designs and processes for gradient systems to meet the requirements for more diverse and challenging applications today and in the future. We focus primarily on soft FGMs based mostly on polymers and their composites because of their increasing need in many emerging technologies that involve soft/hard interfaces, including soft robotics and flexible/wearable electronics.^[31] Please note that the term “soft” in this context is used to include polymers and polymer composites, foams, gels, colloids, as well as most soft biological materials that can be easily deformed by mechanical stresses. In exceptional instances, the discussion delves into hard materials (including hard polymers) because of their relevance to the topic. The review starts with a discussion on the structure and functions of naturally occurring bio-FGMs, using the more notable examples. In a logical manner, we then outline the compositional and structural routes (see Figure 1) used to form manmade FGMs, including those designed to mimic biological examples. This is followed by a brief overview of fabrication techniques for soft polymeric FGMs. Finally, we discuss the challenges and opportunities presented by emerging technologies and potential pathways to develop materials for these needs.

2. Naturally Occurring Bio-FGMs

Bio-FGMs found in animal and plant species have remarkable properties due to complex and often hierarchical designs to meet demanding functional requirements.^[22,24,32,33] Therefore, understanding the mechanisms, processes, and structure-function relationship in biological systems is the key to the design of FGMs for many contemporary engineering problems. The goal is to extract useful engineering principles that can be designed and fabricated within the constraints of contemporary materials and technologies.

2.1. Mechanical Gradient

Bio-FGMs with directionally varying mechanical properties enable various functionalities such as improved load bearing, interfacial strengthening, toughening, adhesion, and contact damage resistance. In animals, FGMs bridge soft to hard tissues and enhance the local mechanical properties in several ways.^[24] For example, the beak of mollusks, such as squids, is made of hard chitin deeply embedded within their soft buccal envelope through a gradual decrease (herein, termed negative gradient) in modulus from the tip to the base of the beak.^[20,33] The gradient occurs due to a corresponding gradual increase (herein, termed positive gradient) in the degree of hydration and a decrease in histidine-rich stiffening protein concentration (Figure 2a). The modulus gradient helps squids during preying by mediating impact force transfer from the stiff beak to the soft tissues of its mouth.^[20] In another mollusk species, the mussel byssus, the gradient hardness within the cuticle structure aids bio-adhesion.^[34,35] The cuticle hardness increases from the proximal region, rich in flexible Pre-COL-P bio-protein (near the mussel body), to the distal region, rich in stiff Pre-COL-D bio-protein (where the cuticle adheres to solid/hard rock), see Figure 2b.

Another example of a modulus gradient is the bone-ligament and bone-tendon joints in humans and other animals for improving fracture and impact resistance at the junction.^[36,37] The gradual increase in local hardness and elastic modulus from tendon/ligament (soft tissue) to bone (hard tissue) due to the increasing degree of mineralization and crystalline order allows the joints to minimize stress concentration by mediating load transfer between the soft and hard tissues (Figure 2c). Examples of mineralization-gradient seen amongst aquatic animals include the ganoid scale of freshwater fishes made of multiple layers exhibiting mineralization gradient to resist biting attacks from predators.^[38,39] In many arthropods, gradient structures help cater to particular requirements, such as the stiffness and

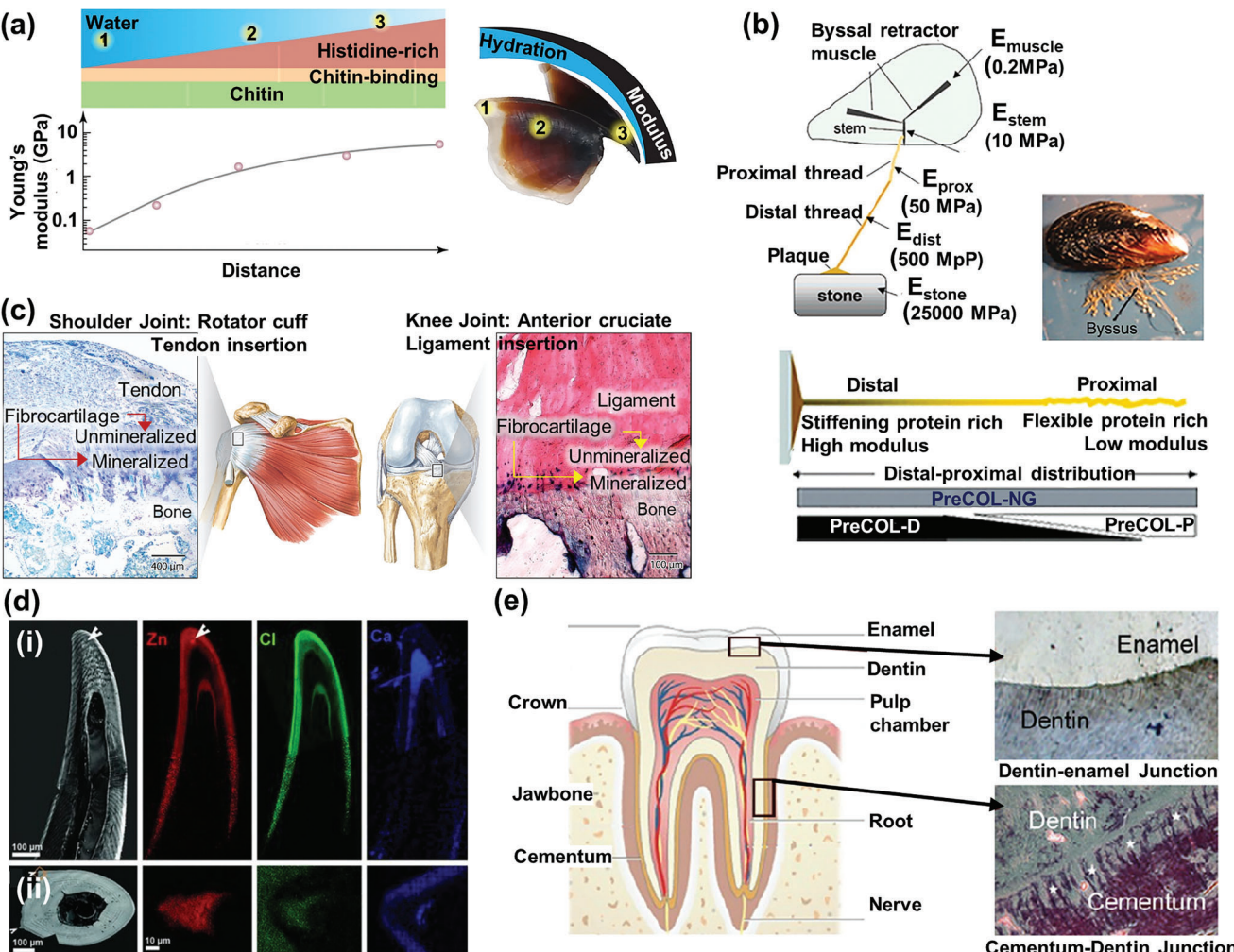


Figure 2. Examples of the mechanical gradient in bio-FGMs via the compositional route a) variation of hydration level (at the top) and Young's modulus along the squid beak (pink circles) as a function of distance from the proximal end of the beak. Adapted with permission.^[33] Copyright 2015, Nature Publishing Group, a division of Macmillan Publishers Limited. All Rights Reserved, b) schematic of a single byssal thread of mussel showing the tenfold increase in stiffness (E_i) between the distal and proximal portions of the thread (top) due to relative variation in protein type from distal to the proximal region (down). Adapted with permission.^[51] Copyright 2023, American Chemical Society, c) the four gradient zones of tendon/ligament-to-bone connections, that is, tendon/ligament, unmineralized fibrocartilage, mineralized fibrocartilage, and bone, where both the mineral content and crystalline ordering increase gradually from tendon/ligament toward the bone. Adapted with permission.^[24] Copyright 2017, Elsevier Ltd. All rights reserved. d) scanning acoustic microscopy images of a longitudinal (top) and cross-sectional (bottom) view of a spider's fang and the corresponding Zn (red), Cl (green), and Ca (Blue) distribution maps from energy-dispersive X-ray spectroscopy measurements. Adapted with permission.^[40] Copyright 2012, WILEY-VCH Verlag GmbH & Co. KGaA, Weinheim, and e) structure of the human tooth and its gradient interfaces: the DEJ and CDJ showing both compositional (gradient mineral concentration) and structural (the collagen fibril orientation, the morphology of mineral crystals) gradient. Adapted with permission.^[24] Copyright 2017, Elsevier Ltd. All rights reserved.

hardness gradient in the venom-injecting fangs of the spiders that enable them to puncture their prey's cuticle made of essentially the same material as the fangs, which is, a chitin-protein composite.^[40,41] This ability comes from the more concentrated distribution of the inorganic ions (zinc, calcium, and chlorine) toward the tip and peripheral regions than the base and core of the fangs, shown in Figure 2d.^[40] This gradient in concentration leads to the variation in the degree of inter-molecular coordination with the protein, thereby causing a gradual increase in stiffness and hardness toward the periphery from the core.^[41] Also, a gradient orientation of chitin fibrils in the protein ma-

trix further induces a positive stiffness gradient from the core to the periphery of the fangs.^[42] Besides spiders, ion distribution-based gradients are found in the high abrasion-resistant jaws of bloodworms, *Glycera dibranchiate*,^[43] adhesive tarsal setae of ladybird beetle,^[44] and the jaws of bristle worms *Nereis virens*,^[45] setae on geckos foot,^[32] etc. The dentin-enamel junction (DEJ) and cementum-dentin junction (CDJ) located in the human tooth also exhibit a gradient in elastic modulus from dentin to enamel and from the cementum to dentin, respectively,^[46,47] see Figure 2e. The gradual transition occurs in the mineral concentration and morphology of mineral crystals, along with a gradient in the

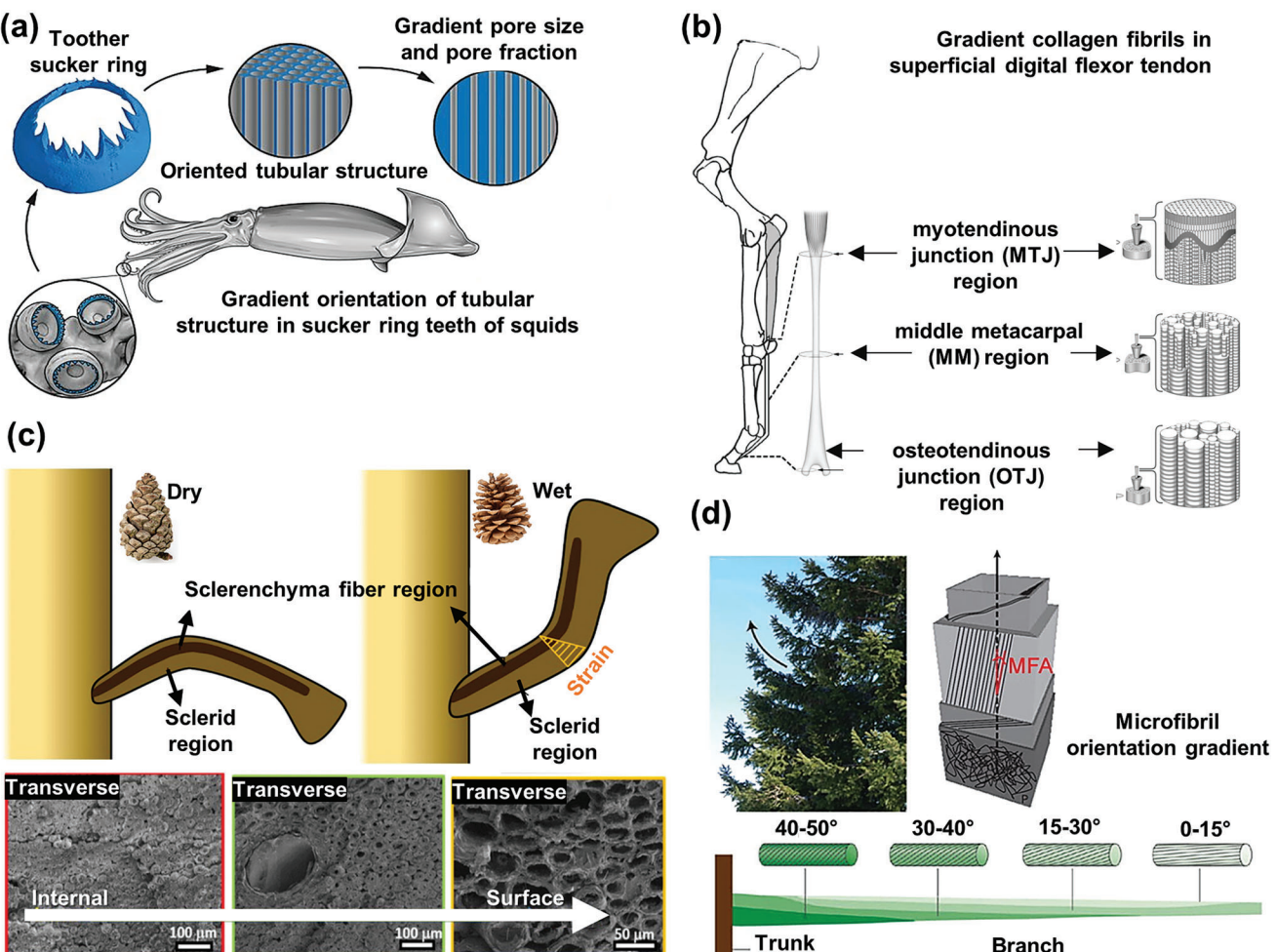


Figure 3. Examples of the mechanical gradient in bio-FGMs via the structural route a) schematic showing the gradient orientation of tubular structures in the sucker ring of squid's tooth that leads to pore size and pore fraction gradient. Adapted with permission.^[69] Copyright 2018, The American Association for the Advancement of Science, b) schematic showing the gradient organization of collagen fibrils in the superficial digital flexor tendon. Adapted with permission.^[58] Copyright 2011, The Authors, Journal of Anatomy, c) deformation of the pine cone scales induced by changes in humidity due to gradient strain originating from the positive porosity gradient that is minimal in the fibrous sclerenchyma region and increases gradually from the inside to the outside surface of the scleroid region. Adapted with permission.^[24] Copyright 2017, Elsevier Ltd. All rights reserved, and d) gradient orientations (microfibril angle MFA) of cellulose microfibrils varying from the lower side of the branch near the trunk to the upper side of the branch. Adapted with permission.^[24] Copyright 2017, Elsevier Ltd. All rights reserved.

collagen fibril orientation, at the DEJ.^[46,47] CDJ demonstrates a chemical composition gradient between cementum and dentin, with the collagen fibers split into individual fibrils and intermingled with the extracellular matrix of mantle dentin.^[46,48] The DEJ and CDJ gradient interface impart excellent toughness and crack-deflecting properties to accommodate mastication (chewing) load while maintaining structural integrity.^[46–50]

Numerous bio-FGMs exhibit a variation in the constituent materials' structural properties, such as porosity, size, morphology, and architecture. The bones in the human body exhibit gradient strength (tensile and compressive) and fracture toughness along the direction of gradual porosity change. In long bones, the external layer, called the cortical bone, is smooth, continuous, and dense ($\rho \approx 1.85 \text{ g cm}^{-3}$). The interior layer called the cancellous bone, has a honeycomb structure and is $\approx 75\text{--}95\%$ porous ($\rho \approx 0.3 \text{ g cm}^{-3}$).^[52] The structure leads to a gradual increase

in stiffness, tensile strength, and fracture toughness from the core to the periphery due to the corresponding gradual decrease in pore size and porosity.^[53–55] In going from a dense external stiff structure to a porous internal one, this bone configuration is an optimized mechanical design, which produces uniform stress distribution with no localized stress. In a similar fashion, the sucker ring teeth in squids consist of an oriented tubular structure with a positive stiffness and hardness gradient from the core to the periphery, corresponding to a negative gradient in pore size or pore volume, as shown in Figure 3a.^[56,57] The gradient provides squids with additional gripping power during prey capture and handling.

Equine's superficial digital flexor tendon at the bone-to-muscle interface shows a gradual increase in elasticity from the myotendinous junction (MTJ) through the middle metacarpal (mM), to the osteotendinous junction (OTJ) as the collagen fibrils

diameter increases from MTJ to mM to OTJ (Figure 3b). While the large fibrils in the OTJ region engender more stiffness to that part of the tendon and make it more stable, the fine fibrils in the MTJ region led to increased elasticity by inhibiting the sliding or creeping amongst themselves than those with large diameters. Thereby leading to an effective dissipation of frictional energy generated between the bone and muscle by gradient fibril distortion.^[58,59] In the plant kingdom, the growth of trees is cyclic. The trunks and branches grow thicker every year as new cells are added beneath the bark, forming tree rings composed of large-lumen and a thin-walled inner layer of cells (earlywood) alternating with narrow-lumen and thick-walled outer layer of cells (latewood).^[21,60,61] The trunk of spruce has a gradient in stiffness originating from the earlywood toward latewood due to a gradual decrease in porosity or gradual increase in fiber density from the earlywood to the latewood or inside out.^[21,60,61] Here, the gradient aids mechanical stability and water transport to the exterior layers of the trunk during the growth period. A positive stiffness gradient is also found in the bamboo stem along the radially outward direction due to a corresponding increase in the vascular bundle density.^[62,63] The scales of pinecones show a gradient distribution of porosity occurring in the outward direction within the cellulose microfibrils-rich scleroid region (Figure 3c). This leads to a strain gradient across the scale when exposed to moisture and allows for reversible opening and closing of the scale for seed dispersion.^[64–66] When warm and dry, dehydration results in the release of the seeds and their dispersal. In another example, gradient orientations of fibrils along the axis of the branches of soft spruce ensure mechanical stability at the trunk-branch junction and help the branches support their weight as they grow,^[66–68] as shown in Figure 3d.

2.2. Optical Gradient

In nature, many species have evolved eyes that use gradient structures to enhance focusing and correct aberrations. Biological species have two kinds of eyes. The camera eye is made of a single lens to focus light on the retina for sharp image formation.^[70] On the other hand, the compound eye consists of numerous repeating units (ommatidia), each of which functions as a separate visual receptor to form either multiple inverted images (apposition eyes) or a single, erect image (superposition eyes).^[70] Light focusing in camera and compound eyes are attributed to the gradient refractive index (GRIN) profile found in their lens and the crystalline cones, respectively.^[22,71–73] Here, we limit the discussion to the GRIN profile of a camera-type lens for brevity. These GRIN lenses constitute thousands of concentric layers of gradually increasing γ -crystallin (eye protein) concentration from the core to the periphery.^[74,75] As summarized in Figure 4a, the refractive index (RI) gradient in the GRIN lens of water-dwelling species (fish, octopus, squid, etc.) is more pronounced than those in air-dwelling species (cow, lion, human, etc.). The slight difference in RI between the environment (water) and the lens of aquatic species renders the cornea almost optically ineffective for focusing light rays on the retina. Thus, in the case of water-dwelling species, most of the optical (focusing) power is derived from the spherical GRIN lens, compensating for the low RI difference to produce sharp images.^[76,77] Without

the GRIN optics, a spherical homogenous lens would still focus light but not at one point along the optical axis, causing image aberration. In contrast, the RI difference between the environment (air) and air-dwellers' lens is significant, and the aspherical GRIN optics helps in the correction of significant geometric aberrations. The largest gradient of RI ($\Delta n \approx 1.12–1.06$) is found in nocturnes that have hemi-ellipsoidal GRIN lens made of a series of ellipsoidal shells with negative RI gradient from the center ($n \approx 1.48–1.42$) toward the periphery ($n \approx 0.36$). This large difference is due to the large size of the GRIN lens, designed to maximize light collection and focus efficiency in the darkness of night.^[78]

Besides its utility in the optical system, GRIN optics is equally helpful for light collection in the spicules of glass sponges *Euplectella Aspergillum* that dwell in the deep dark sea. These sponges can harbor photosynthetically-active phototrophs in the deep tissues of their spicules, indicating the presence of a light transmission system within the spicules to channel ambient light to the phototrophs effectively.^[84,85] The glass spicules have three regions: a solid core of high RI ($\approx 1.45–1.48$), a cylindrical sheath with low RI (≈ 1.425), and the outermost cladding having an oscillating pattern of progressively increasing RI (from 1.433 to 1.438), see Figure 4b.^[80,84] Spatial variation in RI is formed due to corresponding composition variation in the biosilica/organic composite within each spicule resulting in their single- or multi-modal wave-guiding behavior, which is very similar to the commercial optical fibers.^[80,84]

In addition to chemical composition variation, optical bFGMs based on structural manipulations, mainly nanostructural patterns, have been reported.^[2,86–88] For example, in moth eyes, an array of 3D protrusions with dimensions smaller than the wavelength of incident sunlight forms an optical gradient structure that acts like an anti-reflective coating (ARC) to disguise against predators.^[2,81] Light incident on the protrusions or ridges undergoes multiple internal reflections within the crevices resulting in lower net reflection.^[89] A surface with ridges of sub-wavelength dimensions interacts with the light as a single anti-reflective layer, a stepped profile acts as a multilayer ARC, and a tapered profile behaves as an infinite stack of infinitesimally thin layers, introducing a gradual change in refractive index from one medium to the other (Figure 4c).^[81,90] A similar RI gradient is found on the wings of hawkmoths and glasswing butterflies. Here, the irregularly arranged 3D pillars give an optical gradient effect without a sharp, step-like transition between interfacing optical media. As a result, Fresnel reflection losses are minimized, and light transmittance is maximum, causing the wings to be transparent and to function as a camouflage against predators.^[87,88]

Amongst *Pieris* butterflies, the scales of the wings have white pigment, containing beads that scatter light of higher wavelengths. Longitudinal or radial decrease in the density of these pigment-containing beads leads to a gradual reduction in reflectance.^[82,83] In male *Pieris crucivora*, the gradually decreasing density of these granular beads from the tip to the base of the scale leads to a corresponding negative reflectance gradient, as seen in Figure 4d.^[34] Radial gradient reflectance in the wings of *Pieris* white butterflies shows a quasi-random pattern proposed as an optimum design for solar energy concentrators see Figure 4e.^[83]

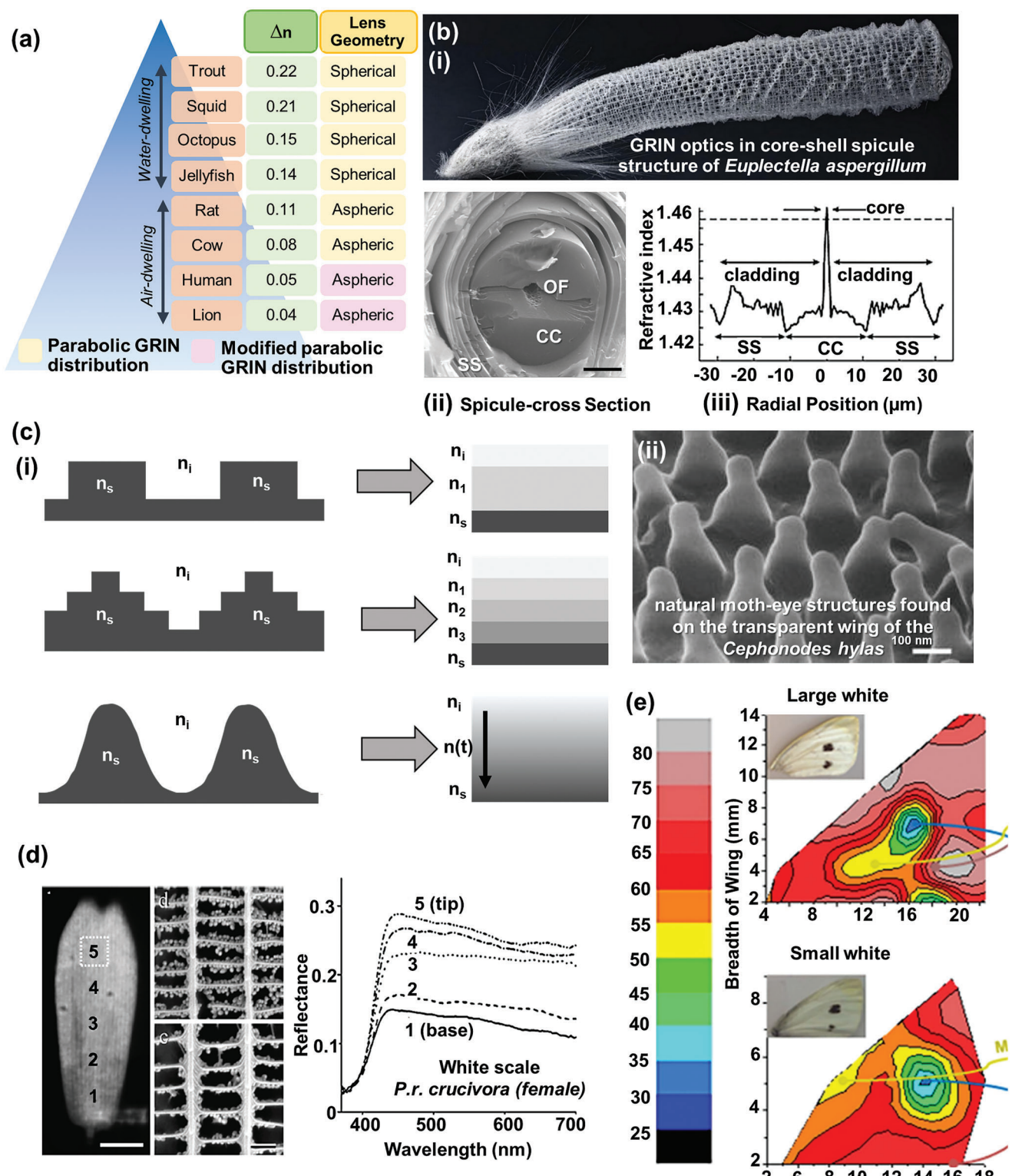


Figure 4. Optical gradient bio-FGMs a) schematic shows the GRIN magnitude and lens geometry difference between water- and air-dwelling animals. Adapted with permission under terms of the Creative Commons Attribution 4.0 (CC BY) Unported License.^[76] Copyright 2013, The Authors, published by SPIE, b) (i) image of glass sponge *Euplectella Aspergillum* with spicules, (ii) single spicule with its core-shell spicule structure: organic filament (OF), central cylinder (CC), and outer striated shell (SS). Adapted with permission under terms of the Creative Commons Attribution 4.0 International^[79] Copyright 2021, The Author(s), published by MDPI, (iii) GRIN profile of an individual spicule along the radius. Adapted with permission.^[80] Copyright 2003, Nature Publishing Group, c) (i) schematic of subwavelength structures like the 3D protrusions found in moth eyes and their analogous refractive

2.3. Other Gradients

Although a vast majority of bio-FGMs are mechanical and optical, a few other property variations amongst biological species are equally noteworthy. For example, in certain fishes, such as the zebrafish, a gradient of electrical coupling, critical for its natural functioning, exists across the developing ventricular myocardium, resulting from the difference in the excitability of the cardiac tissues.^[91] While most gradients are essential for an organism's survival, others may not. For example, the surface polarity gradient in *Morpho* butterflies for selective vapor absorption is a by-product of its scale development process.^[92] The wings of *Morpho* butterflies are decorated with 3D vertical ridges of stacked periodic layers of cuticle and separated by air gaps to form a polarity gradient leading to selective vapor absorption.^[92]

These and other gradient structural elements have each evolved to improve the functioning of biological systems and offer lessons for design standards for biomimetic synthetic materials and methods.

3. Manmade FGMs

Materials are fundamental to modern technologies and manufacturing. Not only are we making use of increasingly diverse materials but also, we are consuming materials more rapidly. FGMs have emerged as a unique class of advanced materials in this context. While the evolutionary design approaches found in nature thus far are numerous (*cf.* Section 2), they are primarily limited to mechanical and optical gradients. On the other hand, engineered FGMs reported in the literature exhibit additional gradient properties such as electrical, magnetic, thermal, acoustic, wettability, etc. Manmade FGMs continue to grow as materials are sought for more advanced and challenging applications. Broadly, the preparation of FGMs is based on two enabling fabrication principles, that is, manipulation of compositional and/or structural features. This section briefly reflects upon the various bioinspired and engineered FGMs based on their designed properties. FGM systems consisting primarily of soft polymers and their composites will be the focus of our discussion.

3.1. Mechanical Gradient

Mechanical gradient materials (MGM) have spatially varied mechanical properties, most often elastic moduli or stiffness. This category of manufactured FGMs constitutes the largest group of FGMs discussed in the literature. Since most MGMs span the continuum of properties between mechanically soft and hard, polymers represent the critical component of almost all known MGMs. Furthermore, literary evidence shows that most man-made MGMs, particularly those having stiffness gradients, are used in tissue engineering applications to achieve various biological functions.^[4,93–98] Some commonly used methods of MGM

preparation include spatial variations in polymer blend volume fraction of the phases,^[99,100] cross-link density,^[99,101,102] degree of crystallization,^[103–105] particle distribution,^[106,107] pore size or porosity distribution,^[93,96] etc.

Spatially varying polymer cross-link density is a common method for preparing MGMs. The underlying principle is to engender higher cross-link density in areas to obtain higher moduli, strength, and dimensional stability while introducing lower cross-link density in other areas to produce more compliant and elastic behavior. Gradient distribution of cross-linking agents results in gradient cross-link density and, thereby gradient mechanical properties. In the case of UV-assisted cross-linking, a gradient is introduced by gradual variation of irradiation intensity either by sliding the photomask or by using a gradient photomask.^[99,101,102] Gradient cross-linking can also be achieved by stereolithography,^[108,109] wherein the gradient UV intensity from top to bottom results in a corresponding decrease in photopolymerization, thereby exhibiting $\approx 100\times$ decrease in the modulus.^[108] The molecular weight of a polymer directly dictates its mechanical properties;^[103,110,111] therefore, an induced molecular weight gradient has been used to prepare MGMs.^[112–114] Wang et al. leveraged the different self-floatability of three different polysiloxane benzophenone photo-initiators to obtain their concentration gradient in a homogenous pre-polymer solution, see Figure 5a.^[112] The positive gradient distribution of the photo-initiator from the bottom to the top of a cylindrical column causes varying degrees of polymerization, thereby rendering a corresponding negative molecular weight gradient from bottom to top.^[112]

Polymers are an indispensable component of soft MGMs and can be easily mixed with solid particles to obtain composites of desirable mechanical properties.^[115–117] Mechanically gradient polymer composite can be prepared by directly controlling the particle content in a gradient fashion to control local properties.^[118] For example, an MGM is fabricated via direct writing, a form of additive manufacturing (AM), by spatio-temporal variation of the relative ratio of cellulose nanofiber (CNF) and polymer matrix, see Figure 5b. As the CNF weight gradually increased, a gradual increase in tensile strength and stiffness, accompanied by a gradual decrease in breaking strain, was observed.^[118] MGMs can also be prepared by gradually varying filler size, distribution, and density in the polymer matrix, which changes the mechanical properties proportionally.^[119–121] In another approach of MGM preparation, gradient distribution of micro-/nano-particles is carried out under an external force field like buoyancy,^[122] magnetic field,^[106,107] electrical field,^[32] centrifugal force,^[123] etc. Wang et al. used a simple technique to remotely distribute magnetic Fe_3O_4 nano-fillers inside a polyurethane acrylate polymer matrix using a magnetic field and mechanical stimuli.^[107] This technique tunes the local stiffness and enables stiff-to-compliant transitions within the micrometer-scale range.^[107] In another study inspired by the setae in the gecko's adhesive feet, Fe_3O_4 -filled PDMS micropillars were

index profiles, as experienced by incident light (top: ridged profile; middle: stepped profile, bottom: tapered profile), (ii) scanning helium ion microscope images of natural moth-eye structures found on the transparent wing of the hawkmoth *Cephonodes hylas*. Reproduced with permission.^[81] Copyright 2012, Springer Science Business Media B.V., d) scales of pierids (male *p. crucivora*) butterflies showing a gradual decrease in reflectance from tip to base (5–1). Adapted with permission.^[82] Copyright 2007, Elsevier Ltd., and e) reflectance gradient in the wings of pierid white butterflies. Adapted under Creative Commons Attribution 4.0 International License^[83] Copyright 2015, The Author(s), published by RSC Publishing.

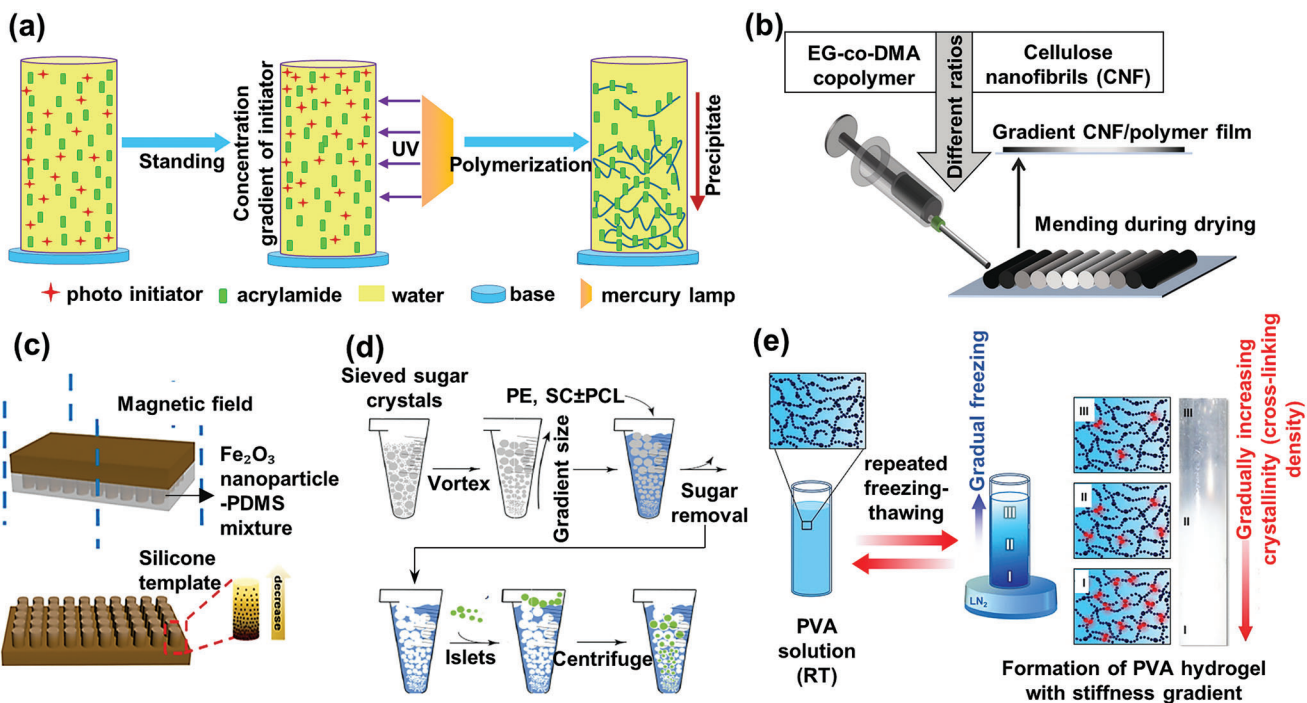


Figure 5. a-c) Manmade mechanical gradient through compositional route a) molecular weight gradient via concentration gradient of self-floatable siloxane-based photo-initiator. Adapted with permission.^[112] Copyright 1999, Royal Society of Chemistry. b) stiffness and breaking strain gradient obtained via direct filament writing of composite hydrogels at varying CNF/EG-co-DMA ratio. Adapted with permission.^[118] Copyright 2016, WILEY-VCH Verlag GmbH & Co. KGaA, Weinheim, c) stiffness gradient induced by the magnetically controlled distribution of ferric nanoparticles in PDMS-based pillar arrays obtained after demolding the composite from the template. Adapted with permission.^[32] Copyright 2023, American Chemical Society, d,e) mechanical gradient through structural variation: d) porosity gradient by gradient porogen size distribution under centrifugal force. Adapted with permission.^[93] Copyright 2020, Wiley Periodicals, Inc., e) gradient unidirectional freezing to obtain crystallinity gradient of poly(vinyl alcohol), PVA hydrogels. Adapted with permission under terms of the Creative Commons Attribution 4.0 International (CC BY 4.0) license.^[124] under Creative Commons Attribution 4.0 International (CC BY 4.0). Copyright 2014, Elsevier Ltd. All rights reserved.

fabricated (Figure 5c). Fabricated under a magnetic field, the negative gradient of filler distribution from bottom to top resulted in a corresponding negative gradient of elastic moduli.^[32] The objective was to prepare dry adhesives with high adhesive strength and long fatigue life.

While compositional gradients in MGMs can be prepared using several different routes, structural MGMs are most commonly created by incorporating porosity gradients in a particular direction within a monolith. Regulating porosity distribution using techniques such as 3D printing^[97,98,125,126] and porogen leaching^[93,96,127] is an effective method of controlling material stiffness and creating robust MGM structures. Porosity gradient, which translates into material density gradient, may enable better load transfer from hard to soft segments.^[96,126,128,129] Another method to prepare MGMs is using the porogen leaching method. It involves size-based segregation similar to the muesli effect, and the porogen undergoes self-organization under a force field. Forget et al. used centrifugal force to redistribute the porogen (dried sucrose micro-particles) based on granular convection to prepare templates, gradually increasing porosity in the vertical direction.^[93] The templates were then infused with a prepolymer solution of different monomers. After curing, the sucrose was leached out, and a biodegradable polymeric scaffold with an increasing porosity in the upward direction was obtained (Figure 5d). The resulting gradient scaffold mimicked the hierar-

chal structure of complex tissue and facilitated the enhanced formation of chondrogenic markers and extracellular matrix compared to non-gradient, uniformly porous scaffolds.^[93] Besides sucrose, gelatin,^[127] salt,^[130] and solvent-dissolvable polymers^[131] have been used to prepare porosity gradients. In certain instances, microfluidics-based gradient bubble distribution has been employed to prepare porosity gradient foams.^[132] Functionally gradient foam (FGF) structures with transverse and axial gradients have been reported to improve the performance of uniform foam-filled collision energy absorbers.^[133] The FGF-filled uniform square tubes,^[134] thin-walled uniform tubes,^[135] and tapered tubes^[136] with foam density varying along axial or transverse directions (see Figure 1c) subjected to impact loading have shown excellent energy absorption capacity under axial and/or lateral impacts. Such FGFs possess larger gradient spans (>10 cm) as compared to other MGMs (\lesssim 20 mm) and have been reported for stand-alone applications rather than in materials interfaces. Another approach to preparing MGMs via the structural route is by tuning the microstructural properties of soft materials like the degree of crystallinity or crystallite size.^[124,137] Kim et al. utilized gradual freezing of poly(vinyl alcohol) PVA solution to create unidirectional transitions in the crystallinity of PVA hydrogels (Figure 5e). The resulting MGM had a positive tensile and compressive moduli gradient from top to bottom, indicating the corresponding positive crystallinity and crystal size gradient.^[124]

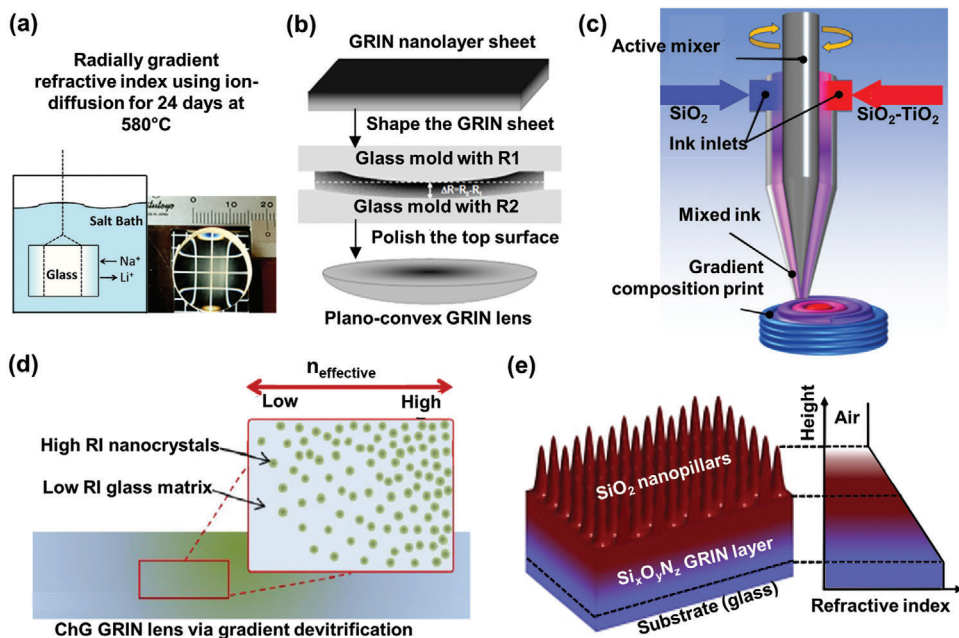


Figure 6. a–c) Manmade optical gradient obtained by composition variation a) sodium (Na^+) for lithium (Li^+) ion exchange in a salt bath is employed to obtain radial gradient in a titania silicate glass. Adapted with permission.^[149] Copyright 2013, Society of Photo-Optical Instrumentation Engineers (SPIE), b) high-temperature, high-pressure molding of forced assembly of a consolidated stack of 40 000 nanolayers of iso-index polymer layers: the GRIN blank approach. Adapted with permission.^[148] Copyright 2006, Wiley Periodicals, Inc., c) direct 3D printing of GRIN lens with titanium as an index-modifying agent. Adapted with permission under terms of Creative Commons Attribution Non-Commercial License 4.0 (CC BY-NC).^[154] Copyright 2020, The Authors, Science Advances. d) optical gradient obtained by (micro-) structural variation: spatially controlled devitrification leading to gradient formation of high RI crystallites in low RI parent glass matrix. Adapted with permission.^[158] Copyright 2016, SPIE, and e) combination of composition variation (in the base) with nano protrusion-induced gradient to prepare GRIN anti-reflection coating. Adapted with permission.^[180] Copyright 2019, Optical Society of America.

3.2. Optical Gradient

In optical gradient materials (OGM), properties such as refractive index (RI), reflectance, transmission, etc., change gradually along one or more dimension(s) due to variations in the composition or structure of the material. An important class of OGM is based on the GRIN optics inspired by the ocular system of living beings with camera-type eyes. As discussed in Section 2.2, they are composed of a single lens with radially varying RI that enables highly focused and aberration-free images, which otherwise would require an array of multiple iso-index lenses. The enhanced focusing power and aberration correction of a single GRIN lens have been employed in the simplification of complex optical instruments such as binoculars,^[10,11] video cameras,^[138] microscopes,^[139,140] etc. Depending on the instrument type, a single GRIN lens can replace 24 to 40 iso-index lenses, thereby avoiding the arduous process of placing and aligning multiple iso-index lenses and cutting down heavily on weight and cost. Besides this, the gradient index profile is utilized in polymer fiber optics for higher bandwidth data transmission^[141–143] and as a multi-modal waveguide.^[144–146]

GRIN lenses are prepared using optically transparent polymers and inorganic glass by occasionally incorporating metallic nanoparticle index-modifying dopants, salts, etc., to obtain a gradient index profile by spatial manipulation of chemical composition. Amongst the polymers, thermoplastics such as poly-methyl methacrylate (PMMA), polystyrene (PS), polycarbonate

(PC), styrene-acrylonitrile copolymer, etc., with RI comparable to glass, are used.^[12,147,148] Fabrication methods such as inter-diffusion,^[149–153] 3D printing,^[154–156] direct laser writing,^[157–161] and molding of GRIN blank^[12,147,162] have been reported. GRIN prepared by inter-diffusion involves either the exchange of ions at the surface of inorganic glass immersed in an ionic bath^[149,150,152] (see Figure 6a), or diffusion of miscible monomers/pre-polymer solutions having different RI,^[12,153,163] respectively. Polymeric OGMs are prepared through several diffusion-based techniques such as diffusion copolymerization,^[153,164,165] extrusion copolymerization,^[166–168] interfacial gel copolymerization,^[169–171] photo-copolymerization,^[146,172,173] centrifugal diffusing polymerization,^[148,166,168] suspension polymerization,^[174,175] etc. For a given set of iso-index materials, the difference in respective RI defines the magnitude of the gradient,^[148,166,168] and the difference in densities determines the direction of the gradient.^[176,177] In a study by Duijnhoven and Bastiaansen, radial OGM was obtained by the spatial distribution of polymers under centrifugal force.^[176] Under high-speed rotation, the high-density, high-RI methyl methacrylate monomer was forced toward the periphery, while the low-density, low-RI styrene monomer remained near the center. Thus, the positive density gradient in the radially outward direction produced a corresponding positive RI gradient directly proportional to the applied rotational speed.^[176] Polymer diffusion, in general, is a facile method to fabricate monolithic axial-, radial-, and spherical-GRIN. In a diffusion-based approach assisted by UV cross-linking of polymers, GRIN was prepared

by varying the degree of cross-linking via spatial variation of UV light intensity.^[173,178,179] The magnitude of the gradient can be further tuned based on the initiator concentration used for cross-linking.^[173]

Additive manufacturing is emerging as a widely used method to create gradient designs. Numerous publications have adopted a variety of additive manufacturing (or 3D printing) to prepare GRIN lenses via co-extrusion,^[147] direct writing,^[154] etc. Polymer co-extrusion technology has been used to stack transparent nanometer-scale-thick iso-index polymer films as an approach to prepare GRIN lenses through GRIN blank (preform).^[147] As shown in Figure 6b, the GRIN lens is obtained by consolidating and molding the GRIN blank between concentric glass molds at high temperatures and pressure.^[147] The final GRIN lens contains $\approx 400\,000$ nanolayers of iso-index polymer. In comparison, biological GRIN lenses are made of tens of thousands of protein layers.^[147] The key advantages of polymer GRIN lenses over inorganic glass GRIN lenses are their lightweight and the ability to easily reproduce aspheric, freeform, and other complex geometric surfaces. However, Dylla-Spears et al. reported that different complex designs were possible in inorganic silica-based GRIN via 3D printing. With an active inline micromixer to prepare a silica nanoparticle lens with varying concentrations of titania as the index-modifying dopant, see Figure 6c. In another method of GRIN preparation, Ocier et al. used direct laser writing as a single-step spherical polymeric GRIN lens fabrication route.^[161] The spatial control of the fill fraction of polymerized negative-tone photoresist inside a porous silicone scaffold was enabled by adjusting the laser power during printing.

In addition to tuning the materials' chemical composition, manipulation of nano- or micro-structures has also been employed to prepare OGMs. For example, inorganic GRIN materials have been prepared by the spatial control of laser irradiation and heat treatment to obtain a gradual variation of crystallinity and crystal size in the chalcogenide glass, Figure 6d.^[157–160] GRIN optics prepared by configuring nanostructures have been widely used to create anti-reflective (AR) surfaces inspired by the sub-wavelength 3D protrusions in moth eyes.^[180–183] In a study by Krauss et al., moth-eye structure and spatial chemical composition variation were combined to obtain a GRIN profile (Figure 6e).^[180]

3.3. Other Gradients

Apart from mechanical and optical gradient materials, many other important attributes can be varied within the bulk of a material to obtain FGMs. To our knowledge, there are few published reports on naturally occurring gradients besides mechanical or optical types, and so is the work on bioinspired artificial soft FGMs with attributes such as electrical, magnetic, etc. However, many engineered FGMs based on soft polymers have been developed over the years to address issues in existing technologies or cater to challenging requirements in specialty applications.

3.3.1. Electrically Gradient Materials

Electrical gradient materials (EGM) have spatially varied electrical properties such as conductivity, permittivity, etc., and can

help improve the performance of electrical devices. Almost all the EGM fabrication routes entail spatial variation of material composition rather than structural tuning. For example, the electrical conductivity gradient was used at the anode/separator interface of lithium-ion batteries (LiB) to suppress the formation of lithium dendrites, which may otherwise cause a short circuit or fire.^[184–187] The positive conductivity gradient from the separator toward the anode of the LiB was obtained by depositing an insulating layer of SiO_2 nanoparticle-embedded CNF, a moderately conductive layer of mixed copper nanowires (CuNW) and CNF, and a highly conductive layer of CuNW, layer by layer on top of each other, see Figure 7a. The assembly provided a gradual through-the-thickness charge-transfer resistance, thereby suppressing the dendrite growth away from the separator and avoiding the risk of a short circuit.^[184] Wang et al. used diffusion under centrifugal force to prepare a radial conductivity gradient wherein high-density carbon fillers were selectively forced toward the periphery of a low-density epoxy matrix.^[188] Besides conductivity, EGM with gradient dielectric permittivity to enhance converse flexoelectric effect under electric potential has also been proposed for sensing, actuation, etc.^[189–191] A ceramic-polymer permittivity gradient composite was prepared by sequential deposition of increasing ceramic particles in a PDMS substrate (Figure 7b).^[192] The resulting permittivity gradient was used to generate an electric field gradient, and hence, a larger deformation was induced by the electric field gradient-induced stress.^[182]

3.3.2. Magnetic Gradient Materials

Magnetic gradient materials (MgGM) display gradually varying magnetic properties, such as magnetization, magnetostriction, coercivity, etc., along one or more directions. They have been used for enhancing the magnetoelectric effect,^[197] imparting self-healing properties,^[198] for magnetically enhanced catalysis,^[199] as an electromagnetic shield (EMS),^[193] etc. Similar to the EGMS, the soft MgGMs can be prepared via a gradually varying distribution of magnetic species within a polymeric matrix under an external force field.^[198] For example, an MgGM was prepared by gradually increasing the filler density of epoxy-based magnetic microcapsules across the thickness of a self-healable, anti-corrosive polymer film under an external magnetic field.^[198] The gradient profile facilitated accelerated healing of the film after physical damage. In another study, a layer-by-layer fabrication technique was employed to obtain gradient loading of conductive fillers in a homogenous iron-filled polyurethane matrix, as shown in Figure 7c.^[193] The resulting dual electrical and magnetic gradient bridged the impedance-matching layer and the highly conductive layer. This led to a particular "absorption-reflection-reabsorption" process, resulting in an EMS with lower reflection and a high shielding effect.^[193]

Structural manipulation of materials, such as porosity variation (as discussed in Section 3.1), is an important enabling route for various FGMS. Gradient porosity has been used for the gradient distribution of functional particles within a composite. In a study by Bahner et al., ultracentrifugation was used to create a gradient-porous template which was subsequently doped with styrene-magnetite magnetic nanoparticles to obtain a gradient particle distribution within an aerogel.^[199] The resulting

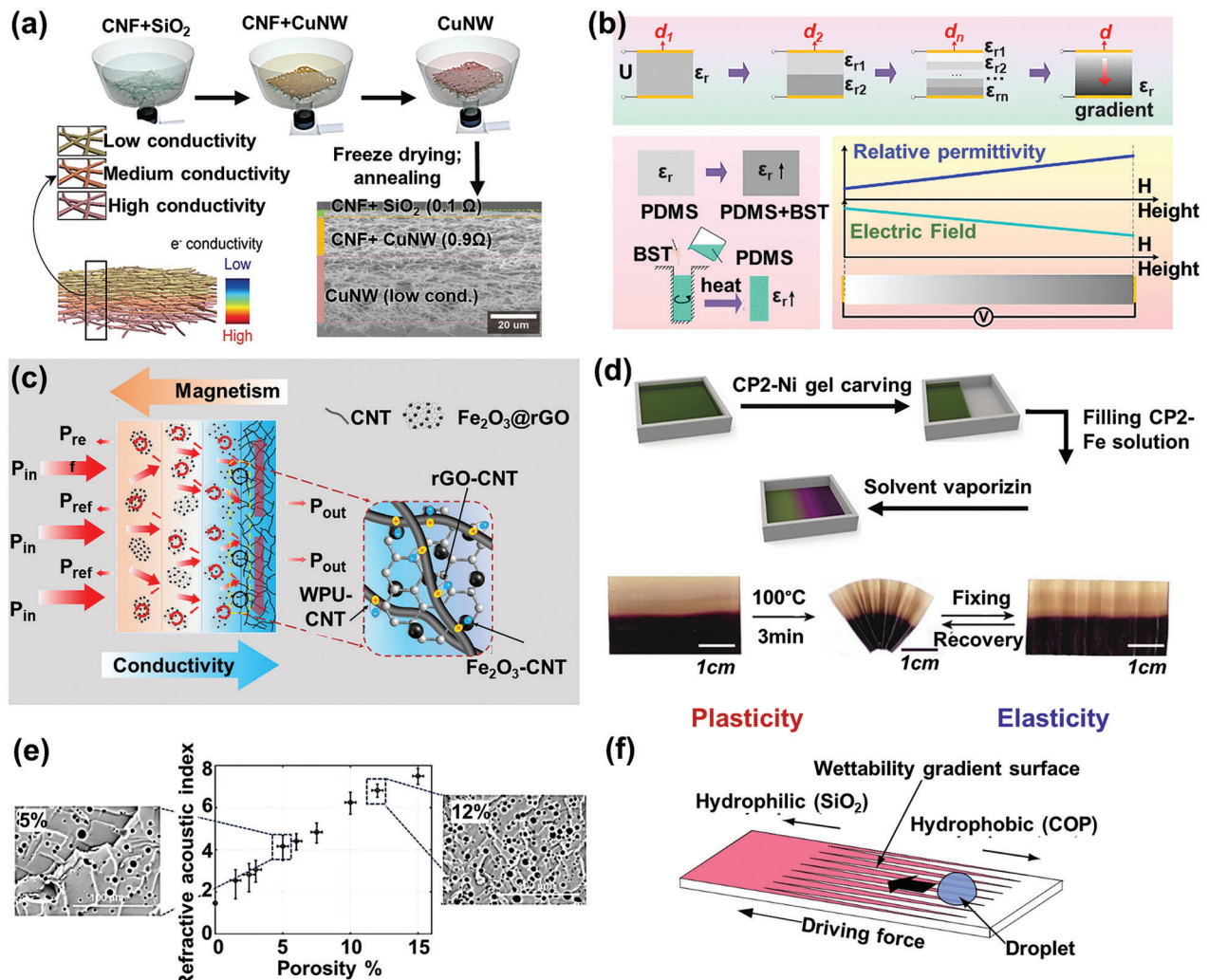


Figure 7. a,b) Manmade electrically gradient materials: a) electrical conductivity gradient host for stable-anode in lithium batteries suppresses the formation of lithium dendrite. Adapted with permission.^[184] Copyright 2020, WILEY-VCH Verlag GmbH & Co. KGaA, Weinheim, b) gradient permittivity dielectric material used to enhance the reverse flexoelectricity effect. Adapted with permission.^[192] Copyright 2019, Rights managed by AIP Publishing, c) dual electrical conductivity and magnetization gradient running opposite each other across a polyurethane-based composite. Adapted with permission.^[193] Copyright 2019, Elsevier Ltd. All rights reserved, d) thermo-mechanical transduction in the polymeric actuator with thermal plasticity gradient produced by controlling the diffusion of two different metal ions during the preparation of a polymer film. Adapted with permission.^[194] Copyright 2017, Wiley-VCH Verlag GmbH & Co. KGaA, Weinheim, e) acoustic gradient refractive index material obtained by the spatial, gradual porosity variation. Adapted with permission under terms of Creative Commons Attribution 4.0 International License^[195] Copyright 2019, The Authors, published by Nature, and f) wettability gradient enabled automatic droplet transportation from the hydrophobic COP side toward the hydrophilic SiO₂ side. Adapted with permission.^[196] Copyright 2015, Rights managed by AIP Publishing.

material exhibited a positive remanence and magnetization gradient along the length corresponding to a positive magnetite concentration gradient. Such an MgGM was proposed for potential application in magnetically enhanced catalysis and magnetic separation.^[199] Besides polymer-based MgGMs, metallic alloys with magnetostrictive gradients and magnetic moment gradients have also been fabricated.^[200–202]

3.3.3. Thermally Gradient Materials

Thermal gradient materials (TGM) have dimensionally varying thermal properties, most often thermal conductivity and ther-

mal coefficient of expansion (CTE), enabling them to bridge hot and cold objects/environments with minimum thermal stress. TGMs have systematically varying material compositions, often along the transverse direction (or through the thickness, see Figure 1c(iii)), with two sides conducive to their respective chemical and physical environments.^[203–206] These are extensively used for high-temperature insulation and load-bearing functions under large temperature gradient conditions in high-temperature turbines,^[207,208] aerospace engines,^[15,16,209] etc. The changing composition leads to a corresponding gradient in thermal conductivity and expansion. It helps mitigate the thermal stress concentration that may cause cracks or delamination at an otherwise sharp interface with CTE mismatch.^[17,210,211]

Polymer-based TGMs employed as thermally insulating materials are prepared via prepegging, molding, and impregnation.^[15,210] The thermal fatigue and range of temperature gradient that TGMs can accommodate depend on their strength, thermal capacity, and CTE of the constituent materials.^[15,210] Hu et al. employed gradient pyrolysis to induce a porosity gradient in a ceramic-silicone prepreg. The multi-layer structure comprised a denser and ceramic-rich top with the least porosity gradually increasing toward the silicone-rich bottom layer. The composite showed an enhanced compressive strength and could serve as a transition material for connecting a high-temperature zone (≥ 1000 °C) with a low-temperature one (≤ 350 °C).^[210] In addition to polymer-based TGMs, gradient thermal barriers made of metals, ceramics, and their composites are also reported.^[204,205] TGMs have also been used for shape reconfiguration in shape memory polymers (SMP).^[14,194,212] Yang et al. prepared an SMP network with gradient ion distribution that possesses a spatial plasticity gradient based on the strong dependence between the metal ions and stress-relaxation kinetics in a metallo-SMP network.^[194] Pre-polymers doped with nickel and iron prepared by free-diffusion and subsequently arrested via cross-linking showed gradient thermal plasticity.^[194] Upon application of heat, the nickel-doped SMP section underwent slow stress relaxation (≈ 60 min), and the iron-doped section showed fast stress relaxation (≈ 4 min), leading to non-uniform contraction and relaxation, thereby allowing fabrication of highly complexed permanent shapes without being limited by traditional molding techniques (Figure 7d). Such shape reconfigurability through spatial control of thermal plasticity may further extend the capabilities of materials into unexplored domains.

3.3.4. Acoustic Gradient Materials

Acoustic gradient materials (AGM) are characterized by a gradual change in acoustic properties such as intensity or speed of sound and acoustic refractive index (aRI), amongst others, in one or more directions. The precise modulation of acoustic properties, along with materials' structural properties, enable the fabrication of acoustic gradient refractive index (aGRIN) lenses,^[213,214] omnidirectional absorbers,^[215,216] sound-focusing devices,^[195,217–219] etc. Gradient aRI meta-materials and metasurfaces have emerged as key routes to manipulating acoustic properties.^[195,220] Especially for high acoustic absorption and low reflection applications, gradient structures can mitigate impedance mismatch between the material and the fluid (air) around it. Structurally, gradient aRI metasurfaces can be obtained by modulating the radii or elastic properties of the inclusions, the lattice spacing or width, etc.^[216,221] Several aGRIN materials are prepared using silicone due to their capability to exhibit a wide range of porosity-tunable acoustic indices.^[195,222] Figure 7e shows a silicone-based AGM wherein the increase in porosity simultaneously increased the aRI, and this attribute was used to prepare soft porous aGRIN metasurfaces with different gradient profiles.^[195] Climente et al. designed a core-shell type omnidirectional absorber (a metamaterial) from small plastic cylinders having progressively decreasing diameters from the inside to the outside of the shell.^[216] Such gradient structures can serve as

gradient-index lenses to focus the acoustic wave into the core, wherein the acoustic energy is dissipated.^[216]

3.3.5. Wettability Gradient Materials

Wettability gradient materials (WGM) have surfaces with spatially varying affinity to liquid in one or more given directions. Such gradient surfaces are useful, for instance, in microfluidic applications,^[196,223] self-cleaning surfaces,^[224,225] tissue engineering,^[226,227] and self-transportation of fluid or analyte in wound dressings.^[228–230] Surface wettability depends primarily on surface-free energy and roughness.^[231,232] The compositional route to create WGMs based on gradually varying surface energy includes gradient chemisorption,^[233–236] vapor diffusion and subsequent chemical reaction on the substrate,^[230,237] and surface modification with irradiation (UV, plasma, corona, electron, and laser beam irradiation, etc.).^[238–242] Zhang et al. prepared an in-plane wettability gradient through the gradual immersion of a gold substrate into a hydrophobic thiol solution for different chemisorption times to produce a gradual transition from hydrophobicity to hydrophilicity.^[233] Other methods of reported surface modification included UV irradiation,^[238,243] electrical discharge,^[239,242,244] and plasma irradiation^[240,244,245] to produce WGMs by selectively modifying the surface chemistry of the substrate. Surface modification methods based on gradient surface patterning or shape gradient^[236,246,247] have also been reported. For instance, a droplet transportation device based on a wettability gradient was prepared by patterning a cycloolefin polymer (COP) plate with a series of alternate COP (hydrophobic) and SiO₂ (hydrophilic) wedge-like patterns, see Figure 7f.^[196] Wettability gradient surfaces produced by combining multiple approaches have been reported.^[248,249] For example, the wettability gradient was obtained by Deng et al. through surface oxidation of a substrate followed by gradient V-shape wedge-patterning.^[249] The resultant WGM enabled controlled droplet transport on a very high adhesion surface, even when the surface was turned upside down. Applying gradient surface roughness (such as fractal roughness, etc.) is also an exciting approach for WGMs.^[246] Other useful fabrication techniques have been thoroughly reviewed in the literature.^[225,250]

3.4. Overview of Fabrication Techniques for Manmade FGMs

The discussion on the various manmade FGMs thus far underlines the need for versatile techniques that allow for precise and controlled fabrication of soft FGMs using mainly polymers and polymer composites. Although we have alluded to various fabrication techniques associated with the FGM designs in our previous discussions, in this section, we would like to cover the broad categories of fabrication currently employed in the fabrication of FGMs in greater detail. The fabrication of metal and ceramic-based FGMs have been classified in the literature in several different ways. While Gupta et al.^[251] chose to use two categories of layer-by-layer construction and mass transport, Zhang et al.^[252] categorized the same into liquid and solid phase approaches. Li et al., on the other hand, proposed two broad categories of bulk processing and coating methods.^[253] Here we

classify the fabrication techniques reported in the literature into four broad categories; additive manufacturing, component redistribution, controlled phase change, and post-modification, see Figure 8. Amongst these, AM is relatively new and more advanced, while the others represent a more traditional approach (herein, termed conventional methods). These fabrication techniques – their capabilities, advantages, and limitations- are discussed here. The desired gradient property and/or geometry, the choice of material, their compatibility with the fabrication process, the energy requirement, and the environmental conditions of the final application are significant in determining the choice of the fabrication technique.

Additive manufacturing (AM) or 3D printing is a process used to directly manufacture 3D objects from their digitally rendered shape data without requiring molds or the need to join or assemble different parts. The transformation of a digital design to a physical object in AM occurs most commonly via layer-by-layer addition of materials to a 3D space. Although AM constitutes a wide array of technologies, the most common are material extrusion,^[256,257] binder jetting,^[258,259] vat photopolymerization,^[260,261] powder bed fusion,^[262,263] directed energy deposition,^[264,265] and sheet lamination.^[266] Evolving technologies based on these fundamental methods are increasingly capable of multi-material processing to produce complex structures and printing with a wider array of soft materials.^[257,267] In some versions of AM, voids and heterogeneity can be designed and may help produce structural FGMs with precision.^[268–270] AM has been used to obtain structural gradients according to a predefined gradient geometry.^[96,98,271,272] The readers are referred to some excellent recent reviews of AM techniques for further details.^[252,253,273] Soft polymeric FGMs can be prepared via AM by spatially varying the material composition^[108,118,192] or by controlling the throughput.^[94,95,257] Figure 8a,b shows some of the applications of AM to fabricate FGMs reported in the literature. The sequential layering of the different components allows controllable tuning of the composition of the layers to obtain fine/continuous^[148,192] or coarse/stepwise^[184] gradients along a given direction. In a type of material extrusion,^[154] described as direct filament writing,^[118] the extrudate with temporally varying composition is deposited in a desired pattern and is used to create FGMs. In general, AM is suitable for fabricating complex shapes with multifunctional properties and offers new opportunities to manufacture novel designs of FGMs.

Gradient fabrication using component redistribution (CR) involves creating a homogenous blend of polymer with another polymer or particulate and subsequently subjecting them to an external force field such as buoyancy,^[122] electric field,^[274] magnetic field,^[32] gravity,^[112] centrifugal force,^[177] convective stretching,^[275] etc. These force fields preferentially drive one or both components to assemble the blend in a gradient fashion. Some of these techniques are illustrated in Figure 8c,d. The spatial gradient distribution is then arrested by cross-linking, curing, or solidification. The CR methods are often used to produce compositional gradients as it allows control of the span and magnitude of the gradient by tuning the intensity or duration of the force field. Interestingly, if the filler particles are replaced with porogenic agents, CR methods can be used to prepare a structural gradient caused by the distribution of pores,^[93,127] see Figure 5d. The most commonly used force fields are magnetic, electric, and

centrifugal because of their simplicity, high controllability, and reliability. However, the major drawback in the field-induced assembly is the enormous energy consumption for a very small gradient span.^[32,274] Also, since redistribution occurs under an external force, in some cases, the risk of reversal of component distribution or homogenization in the absence of the force during use, remains.

Controlled phase change (CPC) refers to the treatment of homogenous parent material with a gradient-inducing stimuli such as gradient thermal, UV, plasma, or laser radiation to create gradient properties, such as elastic modulus^[99,276] or refractive index.^[157,159] The stimuli often cause gradient vitrification^[157,158,124] (Figure 5e) or gradient cross-linking density^[99,276,277] (Figure 8e). This method can be used to prepare both compositional (e.g., cross-linking) and micro-structural (e.g., devitrification) FGMs in either radial^[278] or linear^[158,124] direction. However, it may not support complex gradient designs that can otherwise be produced via AM. The loss of gradient during use via partial or complete homogenization of the material's cross-linking or crystallinity is more probable in FGMs produced via CPC compared to the CR. For example, gradient cross-linking may become volumetrically uniform if consistently exposed to environmental UV light. In most instances, this problem may be mitigated by eliminating residual unpolymerized monomer^[279,280] or crosslinker from the gradient system once the FGMs are fabricated.

Post-modification (PM) is a strategy that involves the formation of a gradient in preformed materials using controlled component diffusion, photopatterning, or laser writing is most often used to produce compositional FGMs (Figure 8f,g). One of the PM approaches is the controlled diffusion of two or more monomers or pre-polymer to generate distributions of molecular components.^[281] While the diffusion-based approach is simple, it is limited to compatible polymers (low interfacial energy and high miscibility).^[281,282] It requires long processing times to create millimeter-scale gradients since the time-scale for pure molecular diffusion scale is proportional to the square of the length span of diffusion.^[283] A relatively faster route involves the temporally-gradual introduction of a substrate into a chemical solution by controlled immersion (gradient chemical reaction^[233] or gradient chemical degradation/etching^[277]) (Figure 8f). Since this process involves the reaction of molecular species, the risk of gradient loss is minimal. Photo-patterning and laser writing are a few other approaches toward post-modification, where chemical changes in the polymer system occur upon reaction with laser radiation.^[161,284,285]

Besides the fabrication techniques mentioned thus far, other process variants also exist. One such process is diffusion-based controlled microfluidic mixing. In this method, a form of continuous deposition of compositionally varying material, produced by mixing the inputs from two or more reservoirs, is used to create a gradient;^[29,286,287] see Figure 8h. Commercially, microfluidic mixing is achieved by available “gradient makers” that continually feed solutions from different reservoirs into a single outlet for deposition and casting in a mold.^[288] In another approach, electrospinning is used for continuous gradient deposition by tuning the process parameters or the composition of input melt (or solution) to obtain compositional^[289,290] or structural^[94,95,98] FGMs. In a typical electrospinning set-up to produce FGMs,

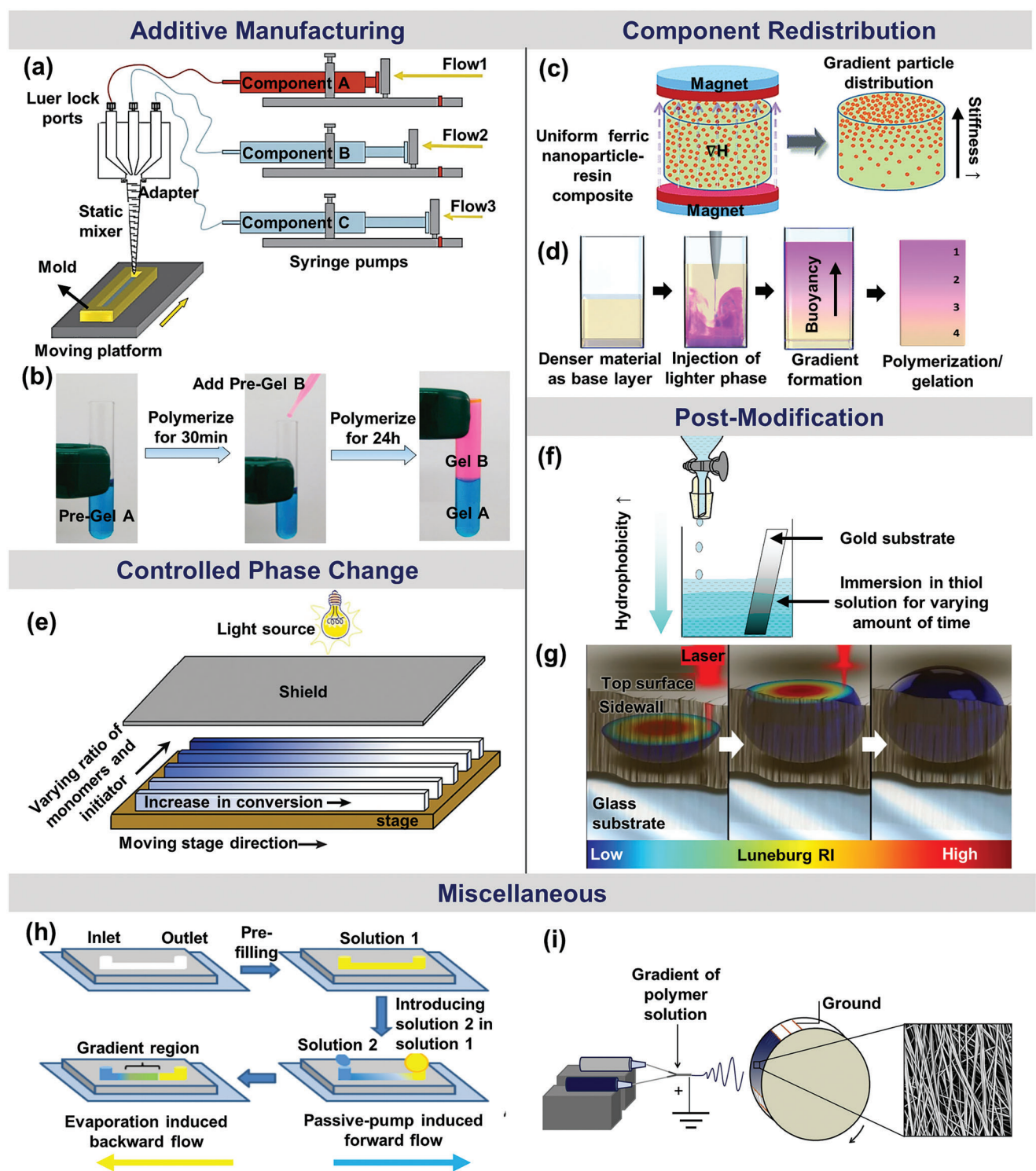


Figure 8. An overview of the broad categories of fabrication techniques used for FGMS: a,b) additive manufacturing: a) 3D printing of a compositional gradient by changing the flow rate of individual components. Adapted with permission.^[100] Copyright 2012, WILEY-VCH Verlag GmbH & Co. KGaA, Weinheim, b) Sequential deposition of different hydrogel mixtures (monomer, cross-linker, initiator, and accelerator) atop one another to create distinct zones of stiffness. Adapted with permission.^[254] Copyright 2023, American Chemical Society, c,d) component redistribution: c) magnetophoresis-induced redistribution of $\text{Fe}_3\text{O}_4@\text{SiO}_2$ nanoparticles inside the resin-nanoparticle composite by applying a magnetic field gradient along the thickness direction. Adapted with permission.^[255] d) buoyancy-driven gradient between materials of different densities to create a biochemical gradient for bio-scaffold. Adapted with permission under Creative Commons CC BY.^[122] Copyright 2019, The Authors, published by WILEY-VCH Verlag GmbH & Co. KGaA, Weinheim, e) controlled phase change: e) gradient conversion of systematically varying unpolymerized mixtures of two dimethylacrylates and camphor quinone initiator system by moving the stage under a shield to gradually increase the irradiation time. Adapted with permission.^[100] Copyright 2012,

the feed material comes from individual reservoirs loaded with different polymer solutions sequentially or from their mixture at varying ratios^[94,95,289,290] (Figure 8i). As such, microfluidic mixing^[29,286,287] and electrospinning^[94,95] are commonly used methods to prepare bio-chemical^[289,290] or porosity^[94,95,98] gradient scaffolds for tissue-engineering applications.

Although soft polymeric FGMs offer great potential in many applications, large-scale industrial manufacturing and commercial applications are still limited,^[291] unlike metal or ceramic-based FGMs, which are more common.^[292–294] Although many of the fabrication processes discussed here are mostly experimental, AM has the most potential. AM can produce complex FGM designs with specific properties through precise control of material compositions and geometric structures at multiple length scales, which are otherwise too time-consuming, expensive, or impossible to manufacture by conventional methods.

4. Needs, Challenges, and Potential Pathways

In this review, we aimed to provide a comprehensive overview of the current understanding of the design principles, structure, and their influence on the key properties of natural and man-made FGMs. We have discussed the fabrication methodologies for manufactured soft FGMs to assess the state of the art in this field and provide insight into future research directions. The continuous or stepwise property variation in the preferred direction makes FGMs suitable for managing stress concentrations and thermal loadings at material interfaces. While robust and well-evolved interfaces between dissimilar materials that are crucial for the proper functioning and survival of plants and animals are plentiful, mitigating interfacial issues in manufactured soft multi-material systems employed in many traditional and emerging technologies remains challenging. Although the bio-FGMs are predominantly mechanical or optical, these include a wealth of instructive design ideas using chemical and structural manipulation of materials. Artificial FGMs reported in the literature, on the other hand, exhibit a wider range of properties than bio-FGMs, such as electrical, magnetic, thermal, acoustic, wettability, etc.

FGMs are inhomogeneous materials with engineered gradients in composition and structure along one or more preferred directions. While FGMs have been used in many commercial applications such as aerospace, automobile, machinery, electronics, optoelectronics, energy, and biomedical fields,^[295] to the best of our knowledge, these applications mostly employ metal and/or ceramic-based hard materials rather than soft polymer-based FGMs. The future need for soft FGMs could be staggering, considering the increasing use of lighter-weight multi-material composites and polymers alongside metals or instead of them in many emerging technologies. For example, soft FGMs could be crucial in designing electrical interconnects in flexible

electronics^[296] and in the emerging fields of human-machine interfaces in numerous wearable and robotic systems that combine soft and rigid materials.^[297] FGMs made of soft polymers, and their composites offer unique functional advantages because of their wide-ranging properties, including mechanical properties, for example, flexibility and conformability. In the published literature, soft FGMs have been reported for various applications, such as interfacial mechanical strengthening via smooth load transfer and efficient energy dissipation from hard to soft segments within a monolith;^[9,32,298] reduction of impedance mismatch between electrically conducting and insulating phases;^[193] reduction in thermal stresses in thermal barriers by efficiently compensating for the CTE mismatch;^[15,299] directional focusing of optical, acoustic, or electromagnetic waves,^[219,220] directional material transport (such as liquid self-transportation^[228] and cellular distribution and proliferation^[7,227,300]), directional material sequestration (such as lithium dendrite in Li-ion battery^[184,185]), stimuli-driven actuation,^[13] etc. In certain applications, FGMs also offer the potential to replace multiple components (such as the combination of iso-index lenses, iso-conductive films, iso-hydrophilic layers, etc.) with an equally functional monolith having added mechanical robustness, thereby enabling simplification of complex instruments such as binoculars,^[10,11] video cameras,^[138] microscopes,^[139,140] etc.

While soft FGMs present enormous opportunities, considerable challenges associated with materials, design, and fabrication methodologies remain, as illustrated in Figure 9. Soft FGMs that have been discussed so far are mostly made of polymer blends,^[149–153] or polymer composites with metallic,^[194,200,201] carbonaceous,^[116,123,188,199] or ceramic fillers^[15,210,301] to attain specific functionalities. A significant challenge in such multi-material systems is the incompatibility of constituent materials, especially polymers, in processing and use. The disparity in material properties such as surface energy (causing high interfacial tension), viscosity, solubility, miscibility, relaxation time, and other rheological, thermal, and mechanical properties may hamper the processing and structural stability of the final FGMs. Even after fabrication, large interfacial tension may cause improper polymer-polymer fusion leading to phase separation (and thereby, altered mechanical properties) at the interface.^[1] For example, the stability of the final structure after processing can be compromised by the mismatch in properties (e.g., CTE or elastic modulus), leading to large residual stresses and mechanical failure.^[302–304] Ensuring compatibility within multi-polymer systems (during and after fabrication) usually involves using a combination of polymers with comparable properties. For instance, in preparing a GRIN lens, PMMA and polycarbonate with similar RI of 1.49 and 1.57, elastic moduli of 3.1 and 2.3 GPa, and densities of 1.19 and 1.2 g cm⁻³ were used, respectively.^[148] Even to prepare GRIN blanks, nanolayered films with low RI difference (≈ 0.0009) of adjacent layers were stacked to maintain

WILEY-VCH Verlag GmbH & Co. KGaA, Weinheim, f,g) post-modification: f) immersion of a gold substrate into thiol solution for different periods of immersion to obtain gradient chemisorption and consequently a hydrophilicity gradient. Adapted with permission.^[233] Copyright 2006, American Chemical Society, g) laser writing of silica used to prepare GRIN by spatial control of gradually varying polymerization. Adapted with permission under terms of Creative Commons Attribution 4.0 International License.^[161] Copyright 2020, The Author(s), published by Springer Nature, h,i) other miscellaneous methods: h) controlled microfluidics mixing to create gradient bio-scaffold. Adapted with permission.^[29] Copyright 2011, Acta Materialia Inc., published by Elsevier Ltd. All rights reserved, i) using electrospinning to deposit material in a layer-by-layer fashion to induce alignment gradient, and thereby corresponding stiffness gradient. Adapted with permission.^[94] Copyright 2016, Acta Materialia Inc., published by Elsevier Ltd. All rights reserved.

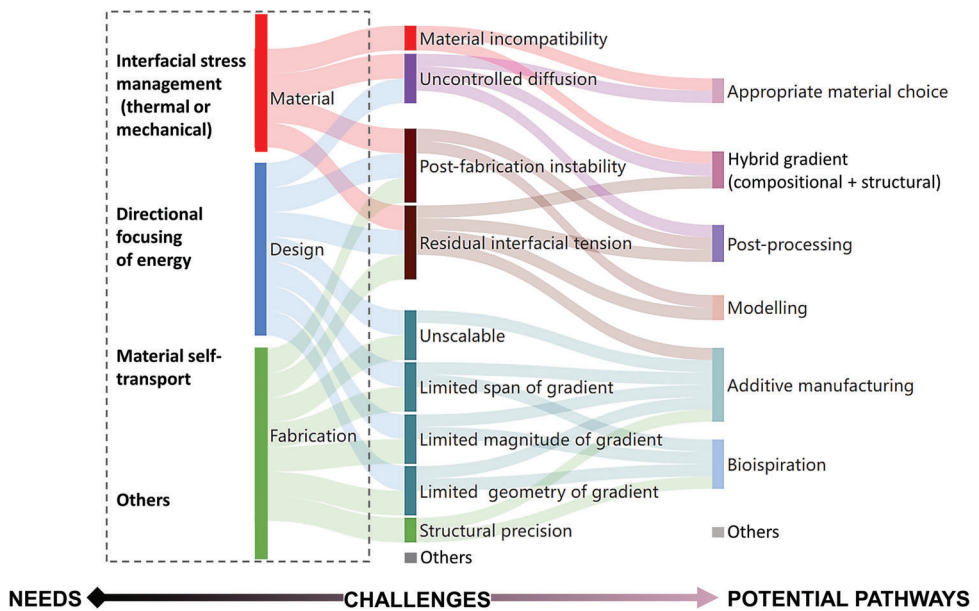


Figure 9. Schematic illustration of the needs, challenges, and potential pathways associated with soft FGMs (left to right). The need for a gradient design falls into three broad categories: material, design, and fabrication. The challenges and potential pathways to their solution relate to these three categories.

the quasi-similar material property as the thickness furthers.^[148] This constraint leads to a narrow set of material choices that translates into a limited gradient magnitude. Sometimes, this may require additional intermediate fabrication steps to realize quasi-similarity between constituents.^[147] Thus, multi-polymer FGM systems that allow for a stable post-fabrication gradient of a larger magnitude and associated fabrication protocols need to be developed. A remedial approach is the use of the same polymer (matrix) infused with volumetrically varying distribution of solid fillers via AM^[118,192] or CR.^[32,123] In doing this, the issues due to polymer-polymer incompatibility are avoided because the gradient property variation becomes solely due to the change in the filler content. However, filler inclusion within a matrix is limited by the upper bound of filler concentration, beyond which the matrix loses its structural integrity.^[305] To get around this issue, other approaches, such as the manipulation of gradient filler orientation,^[94] type,^[306] or size, should be explored.

Fabrication methods play as much of a critical role in achieving the intended gradient characteristics as the constituent materials. The methods of fabrication of soft polymeric FGMs using one or more materials reported in the literature span all broad categories of AM, CR, CPC, and PM, discussed in Section 3.4. These methods can produce distributed location-specific properties with the predetermined transitions in the FGM structure, albeit at varying geometric and microstructural precision. Often the shortcomings of a fabrication method are manifested in its capability to produce either or both of the two critical design parameters of an FGM, the gradient span and magnitude of the gradient (see Section 3.4). Although in most applications discussed in the literature, the gradient span is small and is in the transverse or thickness direction, in many applications, axially-graded FGM structures of larger gradient spans are necessary.^[133–136,307] Most FGM fabrication techniques, however, generally allow for a small gradient span that can be obtained within a reasonable fab-

rication time.^[149,308] For instance, it took 12–24 days to produce a GRIN-lens based on ion diffusion (i.e., component redistribution) of a cylindrical iso-index glass rod of only 1 cm diameter.^[309] The slow fabrication speed is attributed to the slow diffusion, which is proportional to the square of the gradient span.

While a small transverse gradient span is desirable in many current applications (optics, bio-analytics, thermal management, etc.),^[32,168,196] improved fabrication routes are required to prepare FGMs with larger, axial, and directionally complex gradients necessary for newer or advanced applications. In general, complex geometries are either too time-consuming or difficult to manufacture by conventional processes. The limitations originate from the general lack of ability to precisely control process parameters (e.g., rate of diffusion, particle migration in a polymer matrix, etc.).

Another significant issue is associated with the aging of FGMs. Despite the stringent requirements of gradient-forming stimuli modulation in preparing FGMs via conventional processes,^[112,122,124,178] the local volumetric composition and material properties (such as gradient cross-linking density or degree of crystallization) can alter over time due to prolonged environmental exposure and mechanical loading (creep). The gradient characteristics can possibly be further diminished over time because nature drives all systems toward a state of increasing disorder and a thermodynamically low energy state. In the absence of reliable long-term studies on the aging of artificial FGMs, it becomes even more difficult to establish proper post-fabrication management and anti-aging protocols to improve the longevity of FGMs in a given environment. A potential counter strategy to prevent aging-related losses is to adopt structural routes to prepare FGMs. Unlike compositional gradients, structural variations, such as in porosity, cellular design, and others based on filler size and orientation, can be arrested within the bulk of the FGMs as a permanent feature.

Although the gradients of FGMs discussed so far are uniaxial along the transverse or radial direction of the planer, cylindrical, or spherical gradient bodies,^[32,154,185,233] more complex designs may be needed for some applications. One of the more interesting emerging fields of application of FGMs is in complex 3D reprogrammable structures,^[310] with potential applications in biomedical, aerospace, and consumer products, where components are designed and fabricated to morph into multiple configurations during service.^[311–314] Although these fabrication processes are dubbed 4D printing, they are produced through 3D printing, and the object transforms into another shape upon exposure to external stimuli.

Scientific and technological progress in polymer science and technology over the last century expanded from developing a fundamental understanding of polymer morphology and synthesis to the commercial availability of numerous polymers with a wide array of functional properties. But as discussed earlier, using different materials to incorporate different properties within a single monolith with a stable gradient is not simple. Factors such as compatibility, processability, environmental stability, and toxicity are some of the major considerations.

The design of FGM for a given function spans three distinct and interdependent domains: materials, process, and multi-scale structure. Although the underlying parameters in each design domain offer many opportunities to improve and optimize the FGM performance, understanding the complex interactions of a large number of parameters, in particular those involving the nonlinear behavior of polymers, could be challenging. Here, numerical modeling can be a great tool to enable the analysis, characterization, validation, and ultimately optimization of the final structure and the performance of the desired FGMs.^[62,315–318] In general, the current design theories and computer-aided design and modeling tools are primarily intended and used for homogenous and uniform materials and are generally suited for simple geometries and linear material properties. However, almost all FGMs and structures made therefrom consist of at least two phases with continuously varying volume fractions. Thus, advanced numerical models and computational tools capable of rapid and facile simulation of the FGM structure at various scales, material distribution, and ultimately mapping materials-process-structure-property relationships to provide reliable guidelines for designing and constructing application-specific FGMs, are needed. In this regard, voxel-based simulation and design methods have shown great promise for FGMs.^[319,320] It can accommodate heterogeneous materials by designing material compositions and geometrical coordinates separately.^[161,319] Voxel-based methods can also directly interact with certain commercial multi-material 3D printers and are capable of producing FGMs with precise control over the spatial distribution of the material properties.^[320]

In as much as most of the research in the simulation, design, and analysis of gradient structures has focused on those made of traditional hard homogeneous materials (metals and ceramics) with structural gradients.^[321–323] Designing with soft materials, either through the adaptation of existing methods and tools or by developing new modeling and simulation of soft, multi-material-based FGMs, remains an active area of research.

Potential concepts and strategies to solve many of the current challenges in the design of compositional or structural FGMs,

however, can be found in nature. The natural world is full of fantastic design ideas that use a handful of ordinary materials, polysaccharides, proteins, and a few minerals but are designed to fulfill a large number of functions.^[69,324,325] The multifunctionality of the bio-FGMs and systems is rooted in their hierarchical structure, as highlighted in the examples discussed earlier in Section 2. The examples include multi-material-based compositionally and structurally gradient systems of varying magnitude and span with exceptional mechanical and functional properties using simple materials and having properties that surpass those of the individual component materials. For example, bone (collagen and hydroxyapatite) and nacre (protein and aragonite) have far greater toughness than their respective constituents or their homogeneous composites because of their hierarchical structures that range from the atomic and molecular level to the macroscales.^[184,326,327]

Natural materials systems, including the FGMs, evolve (bottom-up) through a slow, quasi-static thermodynamic self-assembly process (or growth) over a long period in a state of internal equilibrium.^[328–330] Mimicking this natural process is beyond the current capability of human engineering. Today's engineering processes are based on a separation of tasks and knowledge fields, from chemistry, materials science, production engineering, and device development all the way to product design, with various selection and assembly processes along this chain. However, a step toward practical bio-inspired design could entail a more integrated interdisciplinary approach with an emphasis on the development of multifunctionality by using fewer materials and their combinations that are structured for specific functions.^[69] This approach is more likely to facilitate a sustainable life-cycle of products while reducing resource and energy usage and environmental emissions. For instance, the tensile and compression strength of the *Saxidomus purpuratus* (mollusk) shell is significantly lower than the abalone nacre, despite having the same aragonite structure.^[331] The lower strength in the former is attributed to a smaller fraction of the organic interlayer. Yet another example is the spicules of glassy sponges with an unusual combination of fracture toughness and optical light propagation properties.^[80,85] This bio-silica with layered structure and compositional is synthesized at extremely low temperatures in the deep sea. Examples like these and many others further emphasize the importance of understanding the structure-centric design of bio-FGMs. The true understanding and adaptation of bio-FGMs are possible by accurate analysis of the system at various length scales. To this end, excellent treatises on bioinspired designs^[324,326,329] are available for the readers' reference.

In conclusion, soft FGMs represent a rapidly developing area of science and engineering and an active area of fundamental and applied research. The many research opportunities in this area are uniquely multidisciplinary and diverse. While problems in computational materials design for gradient structures are challenging, the potential impact could be significant. The hierarchical structural designs in bio-FGM at multi-length scales – from molecular to macro-scale offer many design concepts. Experimental observations and analysis of natural systems guided by theoretical analysis and modeling can open newer avenues to seamlessly integrate materials having very different properties (e.g., hard-to-soft, conductor-to-insulator, etc.), and help integrate materials of entirely different functionalities (e.g.,

thermal actuator-to-thermal sensor; electric conductor-to-electric capacitor, etc.).

Acknowledgements

The authors acknowledge support from N.C. State University's Provost's Fellowship program.

Conflict of Interest

The authors declare no conflict of interest.

Keywords

compositional gradients, soft functionally gradient materials, structural gradients

Received: January 30, 2023

Revised: March 31, 2023

Published online: October 22, 2023

- [1] M. Shen, M. B. Bever, *J. Mater. Sci.* **1972**, *7*, 741.
- [2] S. J. Wilson, M. C. Hutley, *J. Mod. Opt.* **1982**, *29*, 993.
- [3] R. F. Canadas, T. Ren, A. P. Marques, J. M. Oliveira, R. L. Reis, U. Demirci, *Adv. Funct. Mater.* **2018**, *28*, 1804148.
- [4] W. Liu, J. Lipner, J. Xie, C. N. Manning, S. Thomopoulos, Y. Xia, *ACS Appl. Mater. Interfaces* **2014**, *6*, 2842.
- [5] H. K. Min, S. H. Oh, J. M. Lee, G. I. Im, J. H. Lee, *Acta Biomater.* **2014**, *10*, 1272.
- [6] Y. Sun, Y. You, W. Jiang, B. Wang, Q. Wu, K. Dai, *Sci. Adv.* **2020**, *6*, eaay1422.
- [7] Z. Xu, W. Wang, Y. Ren, W. Zhang, P. Fang, L. Huang, X. Wang, P. Shi, *Biomaterials* **2018**, *157*, 125.
- [8] X. Qian, D. Dutta, *Comput.-Aided Des.* **2004**, *36*, 1263.
- [9] D. D. Lima, S. A. Mantri, C. V. Mikler, R. Contieri, C. J. Yannetta, K. N. Campo, E. S. Lopes, M. J. Styles, T. Borkar, R. Caram, R. Banerjee, *Mater. Des.* **2017**, *130*, 8.
- [10] D. S. Kindred, D. T. Moore, *Appl. Opt.* **1988**, *27*, 492.
- [11] J. B. Caldwell, L. R. Gardner, S. N. Houde-Walter, M. T. Houk, D. S. Kindred, D. T. Moore, D. P. Naughton, C. B. Wooley, *Appl. Opt.* **1986**, *25*, 3345.
- [12] A. J. Visconti, K. Fang, J. A. Corsetti, P. McCarthy, G. R. Schmidt, D. T. Moore, *Opt. Eng.* **2013**, *52*, 112107.
- [13] Y. Chen, Z. Chen, C. Chen, H. Ur Rehman, H. Liu, H. Li, M. S. Hedenqvist, *Chem. Eng. J.* **2021**, *421*, 127762.
- [14] F. Ji, X. Liu, D. Sheng, Y. Yang, *Ind. Eng. Chem. Res.* **2019**, *58*, 8090.
- [15] S. Kumar, K. V. V. S. Murthy Reddy, A. Kumar, G. Rohini Devi, *Aerosp. Sci. Technol.* **2013**, *26*, 185.
- [16] W. G. Cooley, A. Palazotto, *Proc. ASME 2005 Int. Mechanical Engineering Congress and Exposition*, American Society of Mechanical Engineers, New York City, USA **2008**, p. 517–526.
- [17] U. Leushake, T. Krell, U. Schulz, *Materialwiss. Werkstofftech.* **1997**, *28*, 391.
- [18] A. Reichardt, A. A. Shapiro, R. Otis, R. P. Dillon, J. P. Borgonia, B. W. Mcenerney, P. Hosemann, A. M. Beese, *Int. Mater. Rev.* **2021**, *66*, 1.
- [19] J. R. Cho, H. J. Park, *J. Mater. Process. Technol.* **2002**, *130-131*, 351.
- [20] A. Miserez, T. Schneberk, C. Sun, F. W. Zok, J. H. Waite, *Science* **2008**, *319*, 1816.
- [21] M. Eder, K. Jungnikl, I. Burgert, *Trees* **2009**, *23*, 79.
- [22] B. K. Pierscionek, J. W. Regini, *Prog. Retinal Eye Res.* **2012**, *31*, 332.
- [23] D. R. Feenstra, R. Banerjee, H. L. Fraser, A. Huang, A. Molotnikov, N. Birbilis, *Curr. Opin. Solid State Mater. Sci.* **2021**, *25*, 100924.
- [24] Z. Liu, M. A. Meyers, Z. Zhang, R. O. Ritchie, *Prog. Mater. Sci.* **2017**, *88*, 467.
- [25] X. Dong, H. Zhao, J. Li, Y. Tian, H. Zeng, M. A. Ramos, T. S. Hu, Q. Xu, *IScience* **2020**, *23*, 101749.
- [26] I. M. El-Galy, B. I. Saleh, M. H. Ahmed, *SN Appl. Sci.* **2019**, *1*, 1378.
- [27] P. S. Ghatare, V. R. Kar, P. E. Sudhagar, *Compos. Struct.* **2020**, *236*, 111837.
- [28] C. Li, L. Ouyang, J. P. K. Armstrong, M. M. Stevens, *Trends Biotechnol.* **2021**, *39*, 150.
- [29] A. Seidi, M. Ramalingam, I. Elloumi-Hannachi, S. Ostrovidov, A. Khademhosseini, *Acta Biomater.* **2011**, *7*, 1441.
- [30] R. M. Mahamood, E. T. Akinlabi, in *Functionally Graded Materials* (Eds: R. M. Mahamood, E. T. Akinlabi), Springer, Cham **2017**, pp. 9–21.
- [31] S. Gong, L. W. Yap, B. Zhu, W. Cheng, *Adv. Mater.* **2020**, *32*, 1902278.
- [32] X. Dong, R. Zhang, Y. Tian, M. A. Ramos, T. S. Hu, Z. Wang, H. Zhao, L. Zhang, Y. Wan, Z. Xia, Q. Xu, *ACS Appl. Polym. Mater.* **2020**, *2*, 2658.
- [33] Y. Tan, S. Hoon, P. A. Guerette, W. Wei, A. Ghadban, C. Hao, A. Miserez, J. H. Waite, *Nat. Chem. Biol.* **2015**, *11*, 488.
- [34] J. H. Waite, E. Vaccaro, C. Sun, J. M. Lucas, *Philos. Trans. R. Soc., B* **2002**, *357*, 143.
- [35] M. J. Harrington, J. H. Waite, *Adv. Mater.* **2009**, *21*, 440.
- [36] B. Wopenka, A. Kent, J. D. Pasteris, Y. Yoon, S. Thomopoulos, *Appl. Spectrosc.* **2008**, *62*, 1285.
- [37] M. Benjamin, H. Toumi, J. R. Ralphs, G. Bydder, T. M. Best, S. Milz, *J. Anat.* **2006**, *208*, 471.
- [38] B. J. F. Bruet, J. Song, M. C. Boyce, C. Ortiz, *Nat. Mater.* **2008**, *7*, 748.
- [39] W. Yang, B. Gludovatz, E. A. Zimmermann, H. A. Bale, R. O. Ritchie, M. A. Meyers, *Acta Biomater.* **2013**, *9*, 5876.
- [40] Y. Politis, M. Prielasser, E. Pippel, P. Zaslansky, J. Hartmann, S. Siegel, C. Li, F. G. Barth, P. Fratzl, *Adv. Funct. Mater.* **2012**, *22*, 2519.
- [41] Y. Politis, E. Pippel, A. C. J. Licuoco-Massouh, L. Bertinetti, H. Blumtritt, F. G. Barth, P. Fratzl, *Arthropod Struct. Dev.* **2017**, *46*, 30.
- [42] B. Bar-On, F. G. Barth, P. Fratzl, Y. Politis, *Nat. Commun.* **2014**, *5*, 3894.
- [43] M. G. Pontin, D. N. Moses, J. H. Waite, F. W. Zok, *Proc. Natl. Acad. Sci. USA* **2007**, *104*, 13559.
- [44] H. Peisker, J. Michels, S. N. Gorb, *Nat. Commun.* **2013**, *4*, 1661.
- [45] H. C. Lichtenegger, T. Schöberl, J. T. Ruokolainen, J. O. Cross, S. M. Heald, H. Birkedal, J. H. Waite, G. D. Stucky, *Proc. Natl. Acad. Sci. USA* **2003**, *100*, 9144.
- [46] S. P. Ho, S. J. Marshall, M. I. Ryder, G. W. Marshall, *Biomaterials* **2007**, *28*, 5238.
- [47] G. W. Marshall, M. Balooch, R. R. Gallagher, S. A. Gansky, S. J. Marshall, *J. Biomed. Mater. Res.* **2001**, *54*, 87.
- [48] S. P. Ho, B. Yu, W. Yun, G. W. Marshall, M. I. Ryder, S. J. Marshall, *Acta Biomater.* **2009**, *5*, 707.
- [49] V. Imbeni, J. J. Krizic, G. W. Marshall, S. J. Marshall, R. O. Ritchie, *Nat. Mater.* **2005**, *4*, 229.
- [50] Y. L. Chan, A. H. W. Ngan, N. M. King, *J. Mech. Behav. Biomed. Mater.* **2011**, *4*, 785.
- [51] J. H. Waite, H. C. Lichtenegger, G. D. Stucky, P. Hansma, *Biochemistry* **2004**, *43*, 7653.
- [52] V. Karageorgiou, D. Kaplan, *Biomaterials* **2005**, *26*, 5474.
- [53] S. Sprio, A. Ruffini, F. Valentini, T. D'alejandro, M. Sandri, S. Panseri, A. Tampieri, *J. Biotechnol.* **2011**, *156*, 347.
- [54] S. J. Simske, R. A. Ayers, T. A. Bateman, *Mater. Sci. Forum* **1997**, *250*, 151.
- [55] S. C. Cowin, G. Gailani, M. Benalla, *Philos. Trans. R. Soc., A* **2009**, *367*, 3401.

- [56] S. H. Hiew, A. Miserez, *ACS Biomater. Sci. Eng.* **2017**, *3*, 680.
- [57] A. Miserez, J. C. Weaver, P. B. Pedersen, T. Schneeberk, R. T. Hanlon, D. Kisailus, H. Birkedal, *Adv. Mater.* **2009**, *21*, 401.
- [58] T. Watanabe, Y. Imamura, D. Suzuki, Y. Hosaka, H. Ueda, K. Hiramatsu, K. Takehana, *J. Anat.* **2012**, *220*, 156.
- [59] T. Watanabe, Y. Imamura, Y. Hosaka, H. Ueda, K. Takehana, *Connect. Tissue Res.* **2007**, *48*, 332.
- [60] T. Speck, I. Burgert, *Annu. Rev. Mater. Res.* **2011**, *41*, 169.
- [61] L. J. Gibson, *J. R. Soc., Interface* **2012**, *9*, 2749.
- [62] E. C. N. Silva, M. C. Walters, G. H. Paulino, *J. Mater. Sci.* **2006**, *41*, 6991.
- [63] M. K. Habibi, A. T. Samaei, B. Gheshlaghi, J. Lu, Y. Lu, *Acta Biomater.* **2015**, *16*, 178.
- [64] C. Dawson, J. F. V. Vincent, A. - M. Rocca, *Nature* **1997**, *390*, 668.
- [65] H. Quan, A. Pirosa, W. Yang, R. O. Ritchie, M. A. Meyers, *Acta Biomater.* **2021**, *128*, 370.
- [66] P. Fratzl, F. G. Barth, *Nature* **2009**, *462*, 442.
- [67] I. Burgert, P. Fratzl, *Philos. Trans. R. Soc., A* **2009**, *367*, 1541.
- [68] I. Burgert, M. Eder, N. Gierlinger, P. Fratzl, *Planta* **2007**, *226*, 981.
- [69] M. Eder, S. Amini, P. Fratzl, *Science* **2018**, *362*, 543.
- [70] E. K. Buschbeck, M. Friedrich, *Evol. Educ. Outreach* **2008**, *1*, 448.
- [71] S. Caveney, P. McIntyre, G. A. Horridge, *Philos. Trans. R. Soc., B* **1981**, *294*, 589.
- [72] V. Lakshminarayanan, M. Kuppuswamy Parthasarathy, *J. Mod. Opt.* **2016**, *0*, 1.
- [73] A. M. Sweeney, D. L. Des Marais, Y.-E. Andrew Ban, S. Johnsen, *J. R. Soc., Interface* **2007**, *4*, 685.
- [74] J. Keenan, D. F. Orr, B. K. Pierscionek, *Mol. Vis.* **2008**, *14*, 1245.
- [75] W. H. Miller, in *Handbook of Sensory Physiology* (Ed: H. Autrum), Springer, Berlin, Heidelberg **1979**, pp. 69–143..
- [76] S. Ji, K. Yin, M. Mackey, A. Brister, M. Ponting, E. Baer, *Opt. Eng.* **2013**, *52*, 112105.
- [77] W. S. Jagger, P. J. Sands, *Vision Res.* **1996**, *36*, 2623.
- [78] L. Schmitz, R. Motani, *Vision Res.* **2010**, *50*, 936.
- [79] A. L. Drozdov, L. A. Zemnukhova, A. E. Panasenko, N. V. Polyakova, A. B. Slobodyuk, A. Y. Ustinov, N. A. Didenko, S. A. Tyurin, *Appl. Sci.* **2021**, *11*, 6587.
- [80] V. C. Sundar, A. D. Yablon, J. L. Grazul, M. Ilan, J. Aizenberg, *Nature* **2003**, *424*, 899.
- [81] S. A. Boden, D. M. Bagnall, in *Encycl. Nanotechnol.* (Ed: B. Bhushan), Springer Netherlands, Dordrecht **2012**, pp. 1467–1477.
- [82] M. A. Giraldo, D. G. Stavenga, *Arthropod Struct. Dev.* **2008**, *37*, 118.
- [83] K. Shanks, S. Senthilarasu, R. H. Ffrench-Constant, T. K. Mallick, *Sci. Rep.* **2015**, *5*, 12267.
- [84] J. Aizenberg, V. C. Sundar, A. D. Yablon, J. C. Weaver, G. Chen, *Proc. Natl. Acad. Sci. USA* **2004**, *101*, 3358.
- [85] F. Brümmer, M. Pfannkuchen, A. Baltz, T. Hauser, V. Thiel, *J. Exp. Mar. Biol. Ecol.* **2008**, *367*, 61.
- [86] D. G. Stavenga, S. Foletti, G. Palasantzas, K. Arikawa, *Proc. R. Soc. B* **2006**, *273*, 661.
- [87] A. Yoshida, M. Motoyama, A. Kosaku, K. Miyamoto, *Zool. Sci.* **1997**, *14*, 737.
- [88] R. H. Siddique, G. Gomard, H. Hölscher, *Nat. Commun.* **2015**, *6*, 6909.
- [89] H. G. Craighead, R. E. Howard, J. E. Sweeney, D. M. Tennant, *J. Vac. Sci. Technol.* **1982**, *20*, 316.
- [90] S. A. Boden, D. M. Bagnall, *Proc. Biomimetics and Bioinspiration*, Vol. 7401, SPIE, Bellingham, WA, USA **2009**, pp. 175–186.
- [91] D. Panáková, A. A. Werdich, C. A. Macrae, *Nature* **2010**, *466*, 874.
- [92] R. A. Potyrailo, T. A. Starkey, P. Vukusic, H. Ghiradella, M. Vasudev, T. Bunning, R. R. Naik, Z. Tang, M. Larsen, T. Deng, S. Zhong, M. Palacios, J. C. Grande, G. Zorn, G. Goddard, S. Zalubovsky, *Proc. Natl. Acad. Sci. USA* **2013**, *110*, 15567.
- [93] A. Forget, D. Rojas, M. Waibel, D. Pencko, S. Gunenthiran, N. Ninan, T. Loudovaris, C. Drogemuller, P. T. Coates, N. H. Voelcker, A. Blencowe, *J. Biomed. Mater. Res., Part B* **2020**, *108*, 2495.
- [94] A. P. Kishan, A. B. Robbins, S. F. Mohiuddin, M. Jiang, M. R. Moreno, E. M. Cosgriff-Hernandez, *Acta Biomater.* **2017**, *56*, 118.
- [95] W. Khoo, S. Chung, S. C. Lim, C. Y. Low, J. M. Shapiro, C. T. Koh, *Mater. Des.* **2019**, *184*, 108184.
- [96] H. Montazerian, M. G. A. Mohamed, M. M. Montazeri, S. Kheiri, A. S. Milani, K. Kim, M. Hoofar, *Acta Biomater.* **2019**, *96*, 149.
- [97] J. E. Trachtenberg, J. K. Placone, B. T. Smith, J. P. Fisher, A. G. Mikos, *J. Biomater. Sci., Polym. Ed.* **2017**, *28*, 532.
- [98] S. Sultan, A. P. Mathew, *Nanoscale* **2018**, *10*, 4421.
- [99] L. G. Major, A. W. Holle, J. L. Young, M. S. Hepburn, K. Jeong, I. L. Chin, R. W. Sanderson, J. H. Jeong, Z. M. Aman, B. F. Kennedy, Y. Hwang, D. - W. Han, H. W. Park, K. - L. Guan, J. P. Spatz, Y. S. Choi, *ACS Appl. Mater. Interfaces* **2019**, *11*, 45520.
- [100] K. U. Claussen, T. Scheibel, H. - W. Schmidt, R. Giesa, *Macromol. Mater. Eng.* **2012**, *297*, 938.
- [101] X. Tong, J. Jiang, D. Zhu, F. Yang, *ACS Biomater. Sci. Eng.* **2016**, *2*, 845.
- [102] Y. Zhang, A. N. Edelbrock, S. J. Rowan, *Eur. Polym. J.* **2019**, *115*, 107.
- [103] G. Perego, G. D. Cella, C. Bastioli, *J. Appl. Polym. Sci.* **1996**, *59*, 37.
- [104] M. K. Joshi, A. P. Tiwari, H. R. Pant, B. K. Shrestha, H. J. Kim, C. H. Park, C. S. Kim, *ACS Appl. Mater. Interfaces* **2015**, *7*, 19672.
- [105] L. E. Nielsen, *J. Appl. Phys.* **1954**, *25*, 1209.
- [106] M. Yan, X. Peng, T. Ma, *J. Alloys Compd.* **2009**, *479*, 750.
- [107] Z. Wang, X. Shi, H. Huang, C. Yao, W. Xie, C. Huang, P. Gu, X. Ma, Z. Zhang, L. - Q. Chen, *Mater. Horiz.* **2017**, *4*, 869.
- [108] A. C. Uzcategui, A. Muralidharan, V. L. Ferguson, S. J. Bryant, R. R. Mcleod, *Adv. Eng. Mater.* **2018**, *20*, 1800876.
- [109] P. Jiang, Y. Zhang, X. Mu, D. Liu, Y. Liu, R. Guo, Z. Ji, X. Wang, X. Wang, *Adv. Mater. Technol.* **2022**, *7*, 2101288.
- [110] W. G. Perkins, N. J. Capiati, R. S. Porter, *Polym. Eng. Sci.* **1976**, *16*, 200.
- [111] C. Tzoganakis, J. Vlachopoulos, A. E. Harnielec, D. M. Shinotsaki, *Polym. Eng. Sci.* **1989**, *29*, 390.
- [112] J. Wang, J. Cheng, J. Liu, Y. Gao, F. Sun, *Green Chem.* **2013**, *15*, 2457.
- [113] F. Sun, N. Zhang, J. Nie, H. Du, *J. Mater. Chem.* **2011**, *21*, 17290.
- [114] F. Sun, Y. Li, N. Zhang, J. Nie, *Polymer* **2014**, *55*, 3656.
- [115] J. P. Greene, in *Automotive Plastics and Composites*, William Andrew Publishing, Norwich, NY, USA **2021**, p. 191–222.
- [116] M. H. Al-Saleh, U. Sundararaj, *Composites, Part A* **2011**, *42*, 2126.
- [117] S. Vigneshwaran, M. Uthayakumar, V. Arumugaprabu, R. Deepak Joel Johnson, *J. Reinf. Plast. Compos.* **2018**, *37*, 1011.
- [118] B. Wang, A. J. Benitez, F. Lossada, R. Merindol, A. Walther, *Angew. Chem. Int. Ed.* **2016**, *55*, 5966.
- [119] T. S. Chow, *J. Mater. Sci.* **1980**, *15*, 1873.
- [120] A. J. Crosby, J. - Y. Lee, *Polym. Rev.* **2007**, *47*, 217.
- [121] F. Kundie, C. H. Azhari, A. Muchtar, Z. A. Ahmad, *J. Phys. Sci.* **2018**, *29*, 141.
- [122] C. Li, L. Ouyang, I. J. Pence, A. C. Moore, Y. Lin, C. W. Winter, J. P. K. Armstrong, M. M. Stevens, *Adv. Mater.* **2019**, *31*, 1900291.
- [123] N. J. Lee, J. Jang, M. Park, C. R. Choe, *J. Mater. Sci.* **1997**, *32*, 2013.
- [124] T. H. Kim, D. B. An, S. H. Oh, M. K. Kang, H. H. Song, J. H. Lee, *Biomaterials* **2015**, *40*, 51.
- [125] L. G. Bracaglia, B. T. Smith, E. Watson, N. Arumugasaamy, A. G. Mikos, J. P. Fisher, *Acta Biomater.* **2017**, *56*, 3.
- [126] Y. Zamani, G. Amoabedin, J. Mohammadi, H. Seddiqi, M. N. Helder, B. Zandieh-Doulabi, J. Klein-Nulend, J. H. Koolstra, *J. Mech. Behav. Biomed. Mater.* **2020**, *104*, 103638.
- [127] G. Tang, H. Zhang, Y. Zhao, Y. Zhang, X. Li, X. Yuan, *J. Biomater. Sci., Polym. Ed.* **2012**, *23*, 2241.

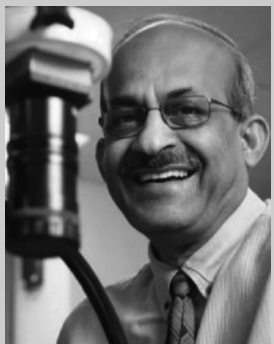
- [128] R. Xiao, X. Feng, R. Fan, S. Chen, J. Song, L. Gao, Y. Lu, *Composites, Part B* **2020**, *193*, 108057.
- [129] J. Svatík, P. Lepcio, F. Ondreáš, K. Zárybnická, M. Zbončák, P. Menčík, J. Jančář, *Polym. Test.* **2021**, *104*, 107405.
- [130] S. Ozkan, D. M. Kalyon, X. Yu, *J. Biomed. Mater. Res.* **2010**, *92A*, 1007.
- [131] C. B. Horner, M. Maldonado, Y. Tai, R. M. I. K. Rony, J. Nam, *ACS Appl. Mater. Interfaces* **2019**, *11*, 45479.
- [132] M. Costantini, J. Jaroszewicz, Ł. Kozoń, K. Szlązak, W. Święszkowski, P. Garstecki, C. Stubenrauch, A. Barbetta, J. Guzowski, *Angew. Chem. Int. Ed.* **2019**, *58*, 7620.
- [133] H. Yin, G. Wen, S. Hou, Q. Qing, *Mater. Des.* **2013**, *44*, 414.
- [134] G. Li, Z. Zhang, G. Sun, F. Xu, X. Huang, *Int. J. Mech. Sci.* **2014**, *89*, 439.
- [135] J. Fang, Y. Gao, G. Sun, Y. Zhang, Q. Li, *Comput. Mater. Sci.* **2014**, *90*, 265.
- [136] H. Yin, G. Wen, H. Fang, Q. Qing, X. Kong, J. Xiao, Z. Liu, *Mater. Des.* **2014**, *55*, 747.
- [137] H. Bai, D. Wang, B. Delattre, W. Gao, J. De Coninck, S. Li, A. P. Tom-sia, *Acta Biomater.* **2015**, *20*, 113.
- [138] M. Deguchi, D. T. Moore, D. S. Kindred, *Image Acquisition and Scientific Imaging Systems*, Vol. 2773, SPIE, Bellingham, WA, USA **1994**, pp. 161–8.
- [139] J. P. Bowen, J. B. Caldwell, L. R. Gardner, N. Haun, M. T. Houk, D. S. Kindred, D. T. Moore, M. Shiba, D. Y. H. Wang, *Appl. Opt.* **1988**, *27*, 3170.
- [140] A. J. Visconti, J. A. Corsetti, K. Fang, P. McCarthy, G. R. Schmidt, D. T. Moore, *Opt. Eng.* **2013**, *52*, 112102.
- [141] T. Ishigure, E. Nihei, Y. Koike, *Appl. Opt.* **1994**, *33*, 4261.
- [142] T. Ishigure, M. Satoh, O. Takanashi, E. Nihei, T. Nyu, S. Yamazaki, Y. Koike, *J. Lightwave Technol.* **1997**, *15*, 2095.
- [143] Y. Koike, T. Ishigure, E. Nihei, *J. Lightwave Technol.* **1995**, *13*, 1475.
- [144] F. Zhang, X. Xu, J. He, B. Du, Y. Wang, *Opt. Lett.* **2019**, *44*, 2466.
- [145] I. Chapalo, A. Theodosiou, K. Kalli, O. Kotov, *J. Lightwave Technol.* **2020**, *38*, 1439.
- [146] Y. Koike, Y. Kimoto, Y. Ohtsuka, *Appl. Opt.* **1982**, *21*, 1057.
- [147] G. Beadie, J. S. Shirk, A. Rosenberg, P. A. Lane, E. Fleet, A. R. Kamdar, Y. Jin, M. Ponting, T. Kazmierczak, Y. Yang, A. Hiltner, E. Baer, *Opt. Express* **2008**, *16*, 11540.
- [148] Y. Jin, H. Tai, A. Hiltner, E. Baer, J. S. Shirk, *J. Appl. Polym. Sci.* **2007**, *103*, 1834.
- [149] A. J. Visconti, J. L. Bentley, *Opt. Eng.* **2013**, *52*, 112103.
- [150] D. S. Kindred, *Appl. Opt.* **1990**, *29*, 4051.
- [151] D. J. Fischer, C. J. Harkrider, D. T. Moore, *Appl. Opt.* **2000**, *39*, 2687.
- [152] K. Shingyouchi, S. Konishi, *Appl. Opt.* **1990**, *29*, 4061.
- [153] Y. Ohtsuka, Y. Terao, *J. Appl. Polym. Sci.* **1981**, *26*, 2907.
- [154] R. Dylla-Spears, T. D. Yee, K. Sasan, D. T. Nguyen, N. A. Dudukovic, J. M. Ortega, M. A. Johnson, O. D. Herrera, F. J. Ryerson, L. L. Wong, *Sci. Adv.* **2020**, *6*, eabc7429.
- [155] A. I. Hernandez-Serrano, M. Weidenbach, S. F. Busch, M. Koch, E. Castro-Camus, *J. Opt. Soc. Am. B* **2016**, *33*, 928.
- [156] S. D. Campbell, D. E. Brocker, D. H. Werner, C. Dupuy, S.-K. Park, P. Harmon, *2015 IEEE Int. Symp. Antennas and Propagation & USNC/URSI National Radio Science Meeting*, IEEE, New York City, USA **2015**, pp. 605–606.
- [157] M. Kang, T. Malendevych, G. Yin, I. B. Murray, M. C. Richardson, J. Hu, I. Mingareev, K. A. Richardson, *Proc. Advanced Optics Imaging Applications UV through LWIR IV*, Vol. 10998, SPIE, Bellingham, WA, USA **2019**, pp. 41–53.
- [158] K. Richardson, A. Buff, C. Smith, L. Sisken, J. D. Musgraves, P. Wachtel, T. Mayer, A. Swisher, A. Pogrebnyakov, M. Kang, C. Pantano, D. Werner, A. Kirk, S. Aiken, C. Rivero-Baleine, *Proc. Advanced Optics for Defense Applications: UV through LWIR*, Vol. 9822, SPIE, Bellingham, WA, USA **2016**, pp. 26–35.
- [159] L. Sisken, *Ph.D. Thesis*, University of Central Florida, Orlando, FL, USA **2017**.
- [160] L. Sisken, M. Kang, J. M. Veras, C. Lonergan, A. Buff, A. Yadav, D. Mcclane, C. Blanco, C. Rivero-Baleine, T. S. Mayer, K. A. Richardson, *Adv. Funct. Mater.* **2019**, *29*, 1902217.
- [161] C. R. Ocier, C. A. Richards, D. A. Bacon-Brown, Q. Ding, R. Kumar, T. J. Garcia, J. Van De Groep, J.-H. Song, A. J. Cyphersmith, A. Rhode, A. N. Perry, A. J. Littlefield, J. Zhu, D. Xie, H. Gao, J. F. Messinger, M. L. Brongersma, K. C. Toussaint, L. L. Goddard, P. V. Braun, *Light: Sci. Appl.* **2020**, *9*, 196.
- [162] D. Gibson, S. Bayya, V. Nguyen, J. Sanghera, M. Kotov, C. McClain, J. Deegan, G. Lindberg, B. Unger, J. Vizgaitis, *Proc. Advanced Optics for Defense Applications: UV through LWIR II*, Vol. 10181, SPIE, Bellingham, WA, USA **2017**, pp. 60–68.
- [163] Y. Koike, Y. Takezawa, Y. Ohtsuka, *Appl. Opt.* **1988**, *27*, 486.
- [164] Y. Ohtsuka, T. Sugano, *Appl. Opt.* **1983**, *22*, 413.
- [165] S. P. Wu, E. Nihei, Y. Koike, *Appl. Opt.* **1996**, *35*, 28.
- [166] W. C. Chen, J. H. Chen, S. Y. Yang, J. Y. Cherng, Y. H. Chang, B. C. Ho, *J. Appl. Polym. Sci.* **1996**, *60*, 1379.
- [167] J.-P. Hsu, S.-H. Lin, *Polymer* **2003**, *44*, 5461.
- [168] K. Yin, S. Ji, H. Fein, M. Ponting, A. Olah, E. Baer, *J. Appl. Polym. Sci.* **2015**, *132*, n/a.
- [169] D.-J. Wang, C.-B. Gu, P.-L. Chen, S.-X. Liu, Z. Zhen, J.-C. Zhang, X.-H. Liu, *J. Appl. Polym. Sci.* **2003**, *87*, 280.
- [170] Y. Koike, E. Nihei, N. Tanio, Y. Ohtsuka, *Appl. Opt.* **1990**, *29*, 2686.
- [171] J.-H. Liu, H.-T. Liu, Y.-B. Cheng, *Polymer* **1998**, *39*, 5549.
- [172] C. F. Jasso, J. Valdez, J. H. Pérez, O. Laguna, *J. Appl. Polym. Sci.* **2001**, *80*, 1343.
- [173] J.-H. Liu, Y.-H. Chiu, *Opt. Lett.* **2009**, *34*, 1393.
- [174] Y. Koike, A. Kanemitsu, Y. Shioda, E. Nihei, Y. Ohtsuka, *Appl. Opt.* **1994**, *33*, 3394.
- [175] Y. Koike, Y. Sumi, Y. Ohtsuka, *Appl. Opt.* **1986**, *25*, 3356.
- [176] D. F. G. H. van, B. CWM, *Appl. Opt.* **1999**, *38*, 1008.
- [177] S. H. Im, D. J. Sun, O. O. Park, H. Cho, J. S. Choi, J. K. Park, J. T. Hwang, *Korean J. Chem. Eng.* **2002**, *19*, 505.
- [178] N. Désilles, L. Lecamp, P. Lebaudy, C. Bunel, *Polymer* **2003**, *44*, 6159.
- [179] H. Esen, C. C. Barghorn, X. Allonas, *Polym. Adv. Technol.* **2016**, *27*, 66.
- [180] M. Kraus, Z. Diao, K. Weishaupt, J. P. Spatz, K. Täschner, H. Bartzsch, R. Schmittgens, R. Brunner, *Opt. Express* **2019**, *27*, 34655.
- [181] Y. Li, J. Zhang, B. Yang, *Nano Today* **2010**, *5*, 117.
- [182] J. Cai, L. Qi, *Mater. Horiz.* **2015**, *2*, 37.
- [183] H. Wang, J. Zhuang, J. Yu, H. Qi, Y. Ma, H. Wang, Z. Guo, *Materials* **2020**, *13*, 5691.
- [184] S.-H. Hong, D.-H. Jung, J.-H. Kim, Y.-H. Lee, S.-J. Cho, S. H. Joo, H.-W. Lee, K.-S. Lee, S.-Y. Lee, *Adv. Funct. Mater.* **2020**, *30*, 1908868.
- [185] J. Pu, J. Li, K. Zhang, T. Zhang, C. Li, H. Ma, J. Zhu, P. V. Braun, J. Lu, H. Zhang, *Nat. Commun.* **2019**, *10*, 1896.
- [186] J. Li, P. Zou, S. W. Chiang, W. Yao, Y. Wang, P. Liu, C. Liang, F. Kang, C. Yang, *Energy Storage Mater.* **2020**, *24*, 700.
- [187] C. Zhang, R. Lyu, W. Lv, H. Li, W. Jiang, J. Li, S. Gu, G. Zhou, Z. Huang, Y. Zhang, J. Wu, Q.-H. Yang, F. Kang, *Adv. Mater.* **2019**, *31*, 1904991.
- [188] Y. Wang, Q.-Q. Ni, Y. Zhu, T. Natsuki, *Polym. Compos.* **2013**, *34*, 1774.
- [189] S. R. Kwon, W. B. Huang, S. J. Zhang, F. G. Yuan, X. N. Jiang, *Smart Mater. Struct.* **2013**, *22*, 115017.
- [190] W. Huang, X. Yan, S. R. Kwon, S. Zhang, F.-G. Yuan, X. Jiang, *Appl. Phys. Lett.* **2012**, *101*, 252903.
- [191] M. Fan, H. Min, *Materials* **2020**, *13*, 1735.
- [192] S. Zhang, K. Liu, X. Wen, T. Wu, M. Xu, S. Shen, *Appl. Phys. Lett.* **2019**, *114*, 052903.
- [193] A. Sheng, W. Ren, Y. Yang, D.-X. Yan, H. Duan, G. Zhao, Y. Liu, Z.-M. Li, *Composites, Part A* **2020**, *129*, 105692.

- [194] L. Yang, G. Zhang, N. Zheng, Q. Zhao, T. Xie, *Angew. Chem.* **2017**, 129, 12773.
- [195] Y. Jin, R. Kumar, O. Poncelet, O. Mondain-Monval, T. Brunet, *Nat. Commun.* **2019**, 10, 143.
- [196] Y. Nakashima, Y. Nakanishi, T. Yasuda, *Rev. Sci. Instrum.* **2015**, 86, 015001.
- [197] C. Lu, P. Li, Y. Wen, A. Yang, C. Yang, J. Yang, W. He, J. Zhang, W. Li, *J. Appl. Phys.* **2014**, 115, 17C726.
- [198] W. Wang, W. Li, W. Fan, X. Zhang, L. Song, C. Xiong, X. Gao, X. Liu, *Chem. Eng. J.* **2018**, 332, 658.
- [199] J. Bahner, N. Hug, S. Polarz, *C* **2021**, 7, 22.
- [200] D. Kan, I. Suzuki, Y. Shimakawa, *J. Appl. Phys.* **2021**, 129, 183902.
- [201] T. Liu, P.-F. Gao, M. Dong, Y.-B. Xiao, Q. Wang, *AIP Adv.* **2016**, 6, 056216.
- [202] H. Yang, Y. Li, M. Zeng, W. Cao, W. E. Bailey, R. Yu, *Sci. Rep.* **2016**, 6, 20427.
- [203] H. Farhat, in *Operation, Maintenance, and Repair of Land-Based Gas Turbines*, Elsevier, Amsterdam, Netherlands **2021**, pp. 63–87.
- [204] L. Łatka, L. Pawłowski, M. Winnicki, P. Sokołowski, A. Małachowska, S. Kożerski, *Appl. Sci.* **2020**, 10, 5153.
- [205] P. G. Lashmi, P. V. Ananthapadmanabhan, G. Unnikrishnan, S. T. Aruna, *J. Eur. Ceram. Soc.* **2020**, 40, 2731.
- [206] A. H. Pakseresht, M. Saremi, H. Omidvar, M. Alizadeh, *Surf. Coat. Technol.* **2019**, 366, 338.
- [207] Krishna Anand VG, K. M. Parammasivam, *J. Therm. Anal. Calorim.* **2021**, 146, 545.
- [208] K. Mondal, L. Nuñez, C. M. Downey, I. J. Van Rooyen, *Ind. Eng. Chem. Res.* **2021**, 60, 6061.
- [209] B. Gleeson, *J. Propul. Power* **2006**, 22, 375.
- [210] Z. Hu, S. Meng, J. Li, W. Xie, J. Niu, Y. Zhou, *Composites, Part A* **2020**, 132, 105799.
- [211] Y. Shinohara, in *Handbook of Advanced Ceramics*, 2nd ed., Academic Press, Oxford **2013**, pp. 1179–1187.
- [212] K. Yu, A. Ritchie, Y. Mao, M. L. Dunn, H. J. Qi, *Procedia IUTAM* **2015**, 12, 193.
- [213] Y. Jin, D. Torrent, Y. Pennec, Y. Pan, B. Djafari-Rouhani, *Sci. Rep.* **2016**, 6, 24437.
- [214] N. Olivier, A. Mermilliod-Blondin, C. B. Arnold, E. Beaurepaire, *Opt. Lett.* **2009**, 34, 1684.
- [215] C. J. Naify, T. P. Martin, C. N. Layman, M. Nicholas, A. L. Thangawng, D. C. Calvo, G. J. Orris, *Appl. Phys. Lett.* **2014**, 104, 073505.
- [216] A. Climente, D. Torrent, J. Sánchez-Dehesa, *Appl. Phys. Lett.* **2012**, 100, 144103.
- [217] A. Climente, D. Torrent, J. Sánchez-Dehesa, *Appl. Phys. Lett.* **2010**, 97, 104103.
- [218] Y. Li, G. Yu, B. Liang, X. Zou, G. Li, S. Cheng, J. Cheng, *Sci. Rep.* **2014**, 4, 6830.
- [219] V. Romero-García, A. Cebrecos, R. Picó, V. J. Sánchez-Morcillo, L. M. García-Raffi, J. V. Sánchez-Pérez, *Appl. Phys. Lett.* **2013**, 103, 264106.
- [220] Y. Xu, Y. Fu, H. Chen, *Nat. Rev. Mater.* **2016**, 1, 16067.
- [221] T. Chen, J. Jiao, D. Yu, *Measurement* **2021**, 171, 108817.
- [222] A. Ba, A. Kovalenko, C. Aristégui, O. Mondain-Monval, T. Brunet, *Sci. Rep.* **2017**, 7, 40106.
- [223] M. S. Maria, P. E. Rakesh, T. S. Chandra, A. K. Sen, *Sci. Rep.* **2017**, 7, 43457.
- [224] D. Li, Z. Wang, D. Wu, G. Han, Z. Guo, *Nanoscale* **2019**, 11, 11774.
- [225] R. Gulfarm, Y. Chen, *Research* **2022**, 2022, 9873075.
- [226] J. H. Lee, S. J. Lee, G. Khang, H. B. Lee, *J. Colloid Interface Sci.* **2000**, 230, 84.
- [227] J.-H. Choe, S. J. Lee, Y. M. Lee, J. M. Rhee, H. B. Lee, G. Khang, *J. Appl. Polym. Sci.* **2004**, 92, 599.
- [228] L. Ni, C. Dietlin, A. Chemtob, C. Croutxé-Barghorn, J. Brendlé, *Langmuir* **2014**, 30, 10118.
- [229] Y.-Y. Song, Z.-P. Yu, L.-M. Dong, M.-L. Zhu, Z.-C. Ye, Y.-J. Shi, Y. Liu, *Langmuir* **2021**, 37, 13703.
- [230] S. Daniel, M. K. Chaudhury, J. C. Chen, *Science* **2001**, 291, 633.
- [231] M. Miyauchi, A. Nakajima, T. Watanabe, K. Hashimoto, *Chem. Mater.* **2002**, 14, 2812.
- [232] W. Zhu, X. Feng, L. Feng, L. Jiang, *Chem. Commun.* **2006**, 2753.
- [233] X. Yu, Z. Wang, Y. Jiang, X. Zhang, *Langmuir* **2006**, 22, 4483.
- [234] J. Mosnáček, A. Popelka, J. Osicka, J. Filip, M. Ilcikova, J. Kollar, A. B. Yousaf, T. Bertok, J. Tkac, P. Kasak, *J. Colloid Interface Sci. J. COLLOID INTERF SCI* **2018**, 512, 511.
- [235] H. Elwing, S. Welin, A. Askendal, U. Nilsson, I. Lundström, *J. Colloid Interface Sci.* **1987**, 119, 203.
- [236] J. Zhang, Y. Han, *Langmuir* **2007**, 23, 6136.
- [237] M. K. Chaudhury, G. M. Whitesides, *Science* **1992**, 256, 1539.
- [238] T. Watanabe, N. Yoshida, *Chem. Rec.* **2008**, 8, 279.
- [239] A. Eifert, J. Petit, T. Baier, E. Bonaccorso, S. Hardt, *Appl. Surf. Sci.* **2015**, 330, 104.
- [240] D. Mangindaan, C.-C. Kuo, S.-Y. Lin, M.-J. Wang, *Plasma Processes Polym.* **2012**, 9, 808.
- [241] A. A. El-Saftawy, A. Elfalaky, M. S. Ragheb, S. G. Zakhary, *Radiat. Phys. Chem.* **2014**, 102, 96.
- [242] B. Wang, X. Wang, H. Zheng, Y. Lam, *Nanomaterials* **2015**, 5, 1442.
- [243] R. Moradpour, E. T. Nassaj, S. H. Tavassoli, T. Parhizkar, M. Ghodsiyan, *J. Nanosci. Nanotechnol.* **2013**, 13, 2247.
- [244] C.-G. Gölander, W. G. Pitt, *Biomaterials* **1990**, 11, 32.
- [245] T.-J. Ko, S. J. Park, M.-S. Kim, S. M. Yoon, S. J. Kim, K. H. Oh, S. Nahm, M.-W. Moon, *Sci. Rep.* **2020**, 10, 874.
- [246] G. McHale, S. J. Elliott, M. I. Newton, N. J. Shirtcliffe, *Contact Angle Wettability and Adhesion*, Vol. 6, 1st ed., CRC Press, London, UK **2009**.
- [247] S. Min, S. Li, Z. Zhu, W. Li, X. Tang, C. Liang, L. Wang, X. Cheng, W.-D. Li, *Microsyst. Nanoeng.* **2020**, 6, 106.
- [248] J. H. Lee, H. G. Kim, G. S. Khang, H. B. Lee, M. S. Jhon, *J. Colloid Interface Sci.* **1992**, 151, 563.
- [249] S. Deng, W. Shang, S. Feng, S. Zhu, Y. Xing, D. Li, Y. Hou, Y. Zheng, *Sci. Rep.* **2017**, 7, 45687.
- [250] S. Morgenthaler, C. Zink, N. D. Spencer, *Soft Matter* **2008**, 4, 419.
- [251] A. Gupta, M. Talha, *Prog. Aeronaut. Sci.* **2015**, 79, 1.
- [252] C. Zhang, F. Chen, Z. Huang, M. Jia, G. Chen, Y. Ye, Y. Lin, W. Liu, B. Chen, Q. Shen, L. Zhang, E. J. Lavernia, *Mater. Sci. Eng. A* **2019**, 764, 138209.
- [253] Y. Li, Z. Feng, L. Hao, L. Huang, C. Xin, Y. Wang, E. Biliti, K. Essa, H. Zhang, Z. Li, F. Yan, T. Peijs, *Adv. Mater. Technol.* **2020**, 5, 1900981.
- [254] S. Gharazi, B. C. Zarket, K. C. Demella, S. R. Raghavan, *ACS Appl. Mater. Interfaces* **2018**, 10, 34664.
- [255] Z. Wang, *Soft Matter* **2019**, 15, 3133.
- [256] R. Sinha, M. Cámara-Torres, P. Scopece, E. Verga Falzacappa, A. Patelli, L. Moroni, C. Mota, *Nat. Commun.* **2021**, 12, 500.
- [257] P. A. G. S. Giachini, S. S. Gupta, W. Wang, D. Wood, M. Yunusa, E. Baharloo, M. Sitti, A. Menges, *Sci. Adv.* **2020**, 6, eaay0929.
- [258] L. Yang, H. Miyanaji, D. Janaki Ram, A. Zandinejad, S. Zhang, *Additive Manufacturing and Strategic Technologies in Advanced Ceramics*, Wiley, Hoboken, NJ, USA **2016**, p. 43–55.
- [259] O. Gülcen, K. Günaydin, A. Tamer, *Polymers* **2021**, 13, 2829.
- [260] S. Nohut, M. Schwentenwein, *J. Manuf. Mater. Process.* **2022**, 6, 17.
- [261] X. Kuang, J. Wu, K. Chen, Z. Zhao, Z. Ding, F. Hu, D. Fang, H. J. Qi, *Sci. Adv.* **2019**, 5, eaav5790.
- [262] J. Zhou, H. Li, Y. Yu, K. Firouzian, Y. Qian, F. Lin, *J. Alloys Compd.* **2020**, 832, 154774.
- [263] J. Zhou, H. Li, Y. Yu, Y. Li, Y. Qian, K. Firouzian, F. Lin, *Mater. Sci. Eng. A* **2020**, 793, 139827.
- [264] M. Ansari, E. Jabari, E. Toyserkani, *J. Mater. Process. Technol.* **2021**, 294, 117117.
- [265] T. Y. Kim, S.-H. Park, K. Park, *Addit. Manuf.* **2021**, 47, 102254.
- [266] Y. Zhang, J. Wang, *Procedia Manuf.* **2017**, 10, 866.

- [267] M. Shusteff, A. E. M. Browar, B. E. Kelly, J. Henriksson, T. H. Weisgraber, R. M. Panas, N. X. Fang, C. M. Spadaccini, *Sci. Adv.* **2017**, 3, eaao5496.
- [268] I. Maskery, A. O. Aremu, L. Parry, R. D. Wildman, C. J. Tuck, I. A. Ashcroft, *Mater. Des.* **2018**, 155, 220.
- [269] A. Seharing, A. H. Azman, S. Abdullah, *Adv. Mech. Eng.* **2020**, 12, 16871402091695.
- [270] S. Y. Choy, C.-N. Sun, K. F. Leong, J. Wei, *Mater. Des.* **2017**, 131, 112.
- [271] H. Zhang, H. Huang, G. Hao, Y. Zhang, H. Ding, Z. Fan, L. Sun, *Adv. Funct. Mater.* **2021**, 31, 2006697.
- [272] S. M. Bittner, B. T. Smith, L. Diaz-Gomez, C. D. Hudgins, A. J. Melchiorri, D. W. Scott, J. P. Fisher, A. G. Mikos, *Acta Biomater.* **2019**, 90, 37.
- [273] K. Chatterjee, T. K. Ghosh, *Adv. Mater.* **2020**, 32, 1902086.
- [274] X.-M. Kong, C.-C. Wu, Y.-R. Zhang, J.-L. Li, *Constr. Build. Mater.* **2013**, 38, 195.
- [275] Y. Du, M. J. Hancock, J. He, J. L. Villa-Uribe, B. Wang, D. M. Cropek, A. Khademhosseini, *Biomaterials* **2010**, 31, 2686.
- [276] J. Dou, S. Mao, H. Li, J.-M. Lin, *Anal. Chem.* **2020**, 92, 892.
- [277] J. Wu, Z. Mao, H. Tan, L. Han, T. Ren, C. Gao, *Interface Focus* **2012**, 2, 337.
- [278] T. Hingant, E. Lavanant, R. Proux, M. Rozé, F. Chevire, Y. Guimond, J. W. Franks, L. Calvez, X.-H. Zhang, *Proc. Advanced Optics for Imaging Applications: UV through LWIR V*, vol. 11403, SPIE, Bellingham, WA, USA **2020**, p. 114030B.
- [279] K. Asano, 浅野健治, I. Kawabuchi, 川渕一朗, Zeon Corp., JP2000264915A **2000**.
- [280] P. H. H. Araújo, C. Sayer, R. Giudici, J. G. R. Poço, *Polym. Eng. Sci.* **2002**, 42, 1442.
- [281] L. M. Cross, K. Shah, S. Palani, C. W. Peak, A. K. Gaharwar, *Nanomed. Nanotechnol. Biol. Med.* **2018**, 14, 2465.
- [282] B. M. Bailey, L. N. Nail, M. A. Grunlan, *Acta Biomater.* **2013**, 9, 8254.
- [283] E. J. Carr, *Phys. Rev. E* **2018**, 97, 042115.
- [284] R. Y. Tam, L. J. Smith, M. S. Shoichet, *Acc. Chem. Res.* **2017**, 50, 703.
- [285] S. A. Fisher, R. Y. Tam, A. Fokina, M. M. Mahmoodi, M. D. Distefano, M. S. Shoichet, *Biomaterials* **2018**, 178, 751.
- [286] J. Idaszek, M. Costantini, T. A. Karlsen, J. Jaroszewicz, C. Colosi, S. Testa, E. Fornetti, S. Bernardini, M. Seta, K. Kasareklo, R. Wrzesieś, S. Cannata, A. Barbetta, C. Gargioli, J. E. Brinchman, W. Świeżkowski, *Biofabrication* **2019**, 11, 044101.
- [287] J. He, Y. Du, J. L. Villa-Uribe, C. Hwang, D. Li, A. Khademhosseini, *Adv. Funct. Mater.* **2010**, 20, 131.
- [288] D. Zhu, X. Tong, P. Trinh, F. Yang, *Tissue Eng. Part A* **2018**, 24, 1.
- [289] X. Zhang, X. Gao, L. Jiang, J. Qin, *Langmuir* **2012**, 28, 10026.
- [290] L. W. Chow, A. Armsgarth, J.-P. St-Pierre, S. Bertazzo, C. Gentilini, C. Aurisicchio, S. D. Mccullen, J. A. M. Steele, M. M. Stevens, *Adv. Healthcare Mater.* **2014**, 3, 1381.
- [291] Graded-Index (GRIN) Multimode Fibers n.d. <https://www.thorlabs.com> (accessed: January 5, 2023).
- [292] S. M. Arnold, M.-J. Pindera, J. Aboudi, Analysis of Plasma-Sprayed Thermal Barrier Coatings With Homogeneous and Heterogeneous Bond Coats Under Spatially Uniform Cyclic Thermal Loading **2003**, <https://ntrs.nasa.gov/citations/20040013220>.
- [293] T. Ricks, S. Arnold, B. Harder, presented at Am. Soc. Composites Tech. Conf., Seattle, WA, USA, September **2018**.
- [294] V. Bhavar, P. Kattire, S. Thakare, S. Patil, R. Singh, *IOP Conf. Ser.: Mater. Sci. Eng.* **2017**, 229, 012021.
- [295] B. Saleh, J. Jiang, R. Fathi, T. Al-Hababi, Q. Xu, L. Wang, D. Song, A. Ma, *Composites, Part B* **2020**, 201, 108376.
- [296] T. Agcayazi, K. Chatterjee, A. Bozkurt, T. K. Ghosh, *Adv. Mater. Technol.* **2018**, 3, 1700277.
- [297] F. Chen, M. Y. Wang, *IEEE Rob. Autom. Mag.* **2020**, 27, 27.
- [298] S. W. Yang, J. Yoon, H. Lee, D. S. Shim, *J. Mater. Res. Technol.* **2022**, 17, 478.
- [299] J. Park, K. Park, J. Kim, Y. Jeong, A. Kawasaki, H. Kwon, *Sci. Rep.* **2016**, 6, 23064.
- [300] J. Genzer, R. R. Bhat, in *Soft Matter Gradient Surfaces: Methods and Applications* (Ed: J. Genzer), John Wiley & Sons, Ltd, Hoboken, NJ, USA **2012**, Ch. 2.
- [301] M. Eldafrawy, J. F. Nguyen, A. K. Mainjot, M. J. Sadoun, *J. Dent. Res.* **2018**, 97, 1324.
- [302] L. G. Zhao, N. A. Warrior, A. C. Long, *Int. J. Solids Struct.* **2006**, 43, 5449.
- [303] J. Jeon, A. Muliana, V. La Saponara, *Compos. Struct.* **2014**, 111, 31.
- [304] M. M. Shokrieh, A. Daneshvar, S. Akbari, *Mater. Des.* **2014**, 53, 209.
- [305] H. J. H. Brouwers, *Phys. Rev. E* **2006**, 74, 031309.
- [306] M. Farahnakian, S. Elhami Joosheghan, M. Moradi, *Mater. Manuf. Process.* **2021**, 36, 301.
- [307] H. Rokni, A. S. Milani, R. J. Seethaler, *J. Mec. Theor. Appl.* **2015**, 49, 26.
- [308] R. Libanori, R. M. Erb, A. Reiser, H. Le Ferrand, M. J. Süess, R. Spolenak, A. R. Studart, *Nat. Commun.* **2012**, 3, 1265.
- [309] S. Ohmi, H. Sakai, Y. Asahara, S. Nakayama, Y. Yoneda, T. Izumitani, *Appl. Opt.* **1988**, 27, 496.
- [310] D. Rus, M. T. Tolley, *Nature* **2015**, 521, 467.
- [311] S. Tibbits, *Archit. Des.* **2014**, 84, 116.
- [312] Z. Ding, C. Yuan, X. Peng, T. Wang, H. J. Qi, M. L. Dunn, *Sci. Adv.* **2017**, 3, 1602890.
- [313] M. Bodaghi, A. R. Damanpack, W. H. Liao, *Mater. Des.* **2017**, 135, 26.
- [314] E. Hajiesmaili, N. M. Larson, J. A. Lewis, D. R. Clarke, *Sci. Adv.* **2022**, 8, eabn9198.
- [315] S. Cao, T. Wang, W. Xu, H. Liu, H. Zhang, B. Hu, W. Yu, *Sci. Rep.* **2016**, 6, 23460.
- [316] Y. Wang, G. Yang, W. Wang, X. Wang, Q. Li, Y. Wei, *Sci. Rep.* **2017**, 7, 10954.
- [317] S. N. Gorb, A. E. Filippov, *Beilstein J. Nanotechnol.* **2014**, 5, 837.
- [318] P. Malik, R. Kadoli, *Ain Shams Eng. J.* **2018**, 9, 149.
- [319] A. O. Aremu, J. P. J. Brennan-Craddock, A. Panesar, I. A. Ashcroft, R. J. M. Hague, R. D. Wildman, C. Tuck, *Addit. Manuf.* **2017**, 13, 1.
- [320] E. L. Doubrovski, E. Y. Tsai, D. Dikovsky, J. M. P. Geraedts, H. Herr, N. Oxman, *Comput.-Aided Des.* **2015**, 60, 3.
- [321] J. Parthasarathy, B. Starly, S. Raman, *J. Manuf. Process.* **2011**, 13, 160.
- [322] E. Sheydaeian, E. Toyserkani, *Int. J. Adv. Manuf. Technol.* **2018**, 96, 3459.
- [323] D. Li, W. Liao, N. Dai, G. Dong, Y. Tang, Y. M. Xie, *Comput.-Aided Des.* **2018**, 104, 87.
- [324] B. Bhushan, *Philos. Trans. R. Soc., A* **2009**, 367, 1445.
- [325] K.-J. Cho, J.-S. Koh, S. Kim, W.-S. Chu, Y. Hong, S.-H. Ahn, *Int. J. Precis. Eng. Manuf.* **2009**, 10, 171.
- [326] U. G. K. Wegst, H. Bai, E. Saiz, A. P. Tomsia, R. O. Ritchie, *Nat. Mater.* **2015**, 14, 23.
- [327] H. Sun, Y. Li, S. Yu, J. Liu, *Front. Bioeng. Biotechnol.* **2020**, 8, 00295.
- [328] J. Peterson, *Am. Biol. Teach.* **2012**, 74, 22.
- [329] D. J. Kushner, *Bacteriol. Rev.* **1969**, 33, 302.
- [330] G. M. Whitesides, B. Grzybowski, *Science* **2002**, 295, 2418.
- [331] W. Yang, G. P. Zhang, X. F. Zhu, X. W. Li, M. A. Meyers, *J. Mech. Behav. Biomed. Mater.* **2011**, 4, 1514.



Akanksha Pragya received her B.Tech. in Textile Technology from the Indian Institute of Technology in New Delhi (2019) and is presently a Ph.D. student in the Fiber & Polymer Science program at North Carolina State University. She is currently working in the area of functionally gradient materials for e-textile applications.



Tushar K. Ghosh is the William A. Klopman Distinguished Professor of Textiles at the Wilson College of Textiles at North Carolina State University. He received his B.Sc. Tech. degree in textile technology from the University of Calcutta (1975), M. Tech. degree in textile engineering from the Indian Institute of Technology in New Delhi (1978), and a Ph.D. in fiber and polymer science (1987) from North Carolina State University. His diverse research interests include textile processes, mechanics of fibrous structures, design, and development of functional textiles. His current research focuses on fiber-based sensors and actuators involving polymer nanocomposites, adaptive and responsive electronic textiles, electroactive polymers, and biomimetic systems.